

Synthesis and Structure-Activity Relationships of Pyrazole-based Inhibitors of Meprin α and β

Kathrin Tan^[a], Christian Jäger^[b], Stefanie Geissler^[a], Dagmar Schlenzig^[a], Mirko Buchholz^[a,c], Daniel Ramsbeck^{[a]}*

AUTHOR ADDRESS

^[a] Fraunhofer Institute for Cell Therapy and Immunology IZI, Department of Drug Design and Target Validation MWT, Biocenter, Weinbergweg 22, 06120 Halle (Saale), Germany

^[b] Vivoryon Therapeutics N.V., Weinbergweg 22, 06120 Halle (Saale), Germany

^[c] present address: PerioTrap Pharmaceuticals GmbH, Weinbergweg 22, 06120 Halle (Saale), Germany

*Corresponding Author E-mail: daniel.ramsbeck@izi.fraunhofer.de Phone: +49 3451314 2826

KEYWORDS

Meprin, metalloprotease, hydroxamate, inhibitor, pyrazole

ABSTRACT

Targeting metalloproteinases has been in focus of drug design for a long time. However, human proteinases of the astacin family, in particular meprin α and β emerged as potential drug targets just recently. More and more data links them to several diseases with different pathological background. Nevertheless, the validation of meprins as suitable drug targets requires highly potent and selective inhibitors as chemical probes to elucidate their role in pathophysiology. Albeit highly selective inhibitors of meprin β have already been reported, only inhibitors of meprin α with modest activity or selectivity are known. Starting from recently reported heteroaromatic scaffolds, the aim of this study was the optimization of meprin α and/or meprin β inhibition while keeping the favorable off-target inhibition profile over other metalloproteases. We now report novel potent pan-meprin inhibitors as well as highly active inhibitors of meprin α with superior selectivity over meprin β . The latter are suitable to serve as chemical probes and enable further target validation of meprin proteases.

Introduction

The metalloproteases meprin α and β are potentially involved in the pathophysiology of various diseases. Thus, they emerged as promising drug targets during the last years. Meprin α is supposed to act as promigratory protease in the context of colorectal and hepatocytic cancer¹⁻⁶ and was also linked to vascular diseases like arteriosclerosis, cardiac remodeling and aneurysms, recently⁷⁻⁹. Meprin β is also involved in cancer cell invasion^{10,11} and moreover is able to act as an alternative beta-secretase, contributing to the progression of Alzheimer's disease via the release of neurotoxic amyloid peptides¹²⁻¹⁷. Both proteases act as procollagenases and are involved in the biosynthesis and assembly of collagen fibrils. Hence, they are potentially involved in the development of fibrotic diseases, e.g. keloids or lung fibrosis.¹⁸⁻²⁰ Further substrates include different cytokines and components of the extracellular matrix, rendering meprin α and β potential drug targets in inflammatory or kidney diseases.²¹⁻²⁷

The abovementioned roles in pathophysiology suggest meprin α and β as valuable drug targets, but further target validation is needed to shed light on their individual contribution to the onset of diseases and potential treatment options. For this purpose, highly potent and selective inhibitors are required that could serve as lead compounds for preclinical development and/or chemical probes to elucidate the impact of pharmacological modulation of meprin activity on disease progression. However, no inhibitor of either meprin α or β has entered clinical trials, yet. Nevertheless, potent inhibitors of both isoenzymes are already known (Figure 1). The first inhibitors of meprins have been reported by Kruse et al., e.g. the naturally occurring Actinonin (**1**) or the broad spectrum metalloprotease inhibitor NNGH (**4a**).²⁷ Later, novel chemotypes have been identified by high throughput screening (**2** and **3**).²⁸ The first systemic elaboration of structure-activity relationship using NNGH as lead structure led to the development of potent sulfonamide (**4b**) and tertiary amine based inhibitors (**5a,b**).²⁹⁻³¹ The latter exhibit favorable inhibition of either meprin β or α , respectively, and moreover a superior selectivity profile against off-target metalloproteases. This is a prerequisite for further development, since unselective inhibition of off-target proteases could lead to undesired side effects and thus impair a potential clinical application.³² The SAR of the sulfonamide and tertiary amine based inhibitors revealed the importance of an acidic scaffold decoration to achieve potent inhibition of meprin β .^{29,33} This corroborates its substrate

specificity, with a high preference of acidic amino acids in P1 and P1'-position of the respective substrates. This is mediated by a cluster of positively charged arginine residues in the active site cleft, forming the S1, S1' and S2' pocket, respectively.³⁴ Although the S1'-pocket in meprin α comprises an arginine as well, the prevalence for acidic substrates is less pronounced, due to differing amino acids shaping the S1 and S2' pockets, i.e. tyrosine residues^{34,35}. This also translates into the structural requirements for meprin α inhibitors, being less acidic and also neutral moieties could lead to sufficient activity.

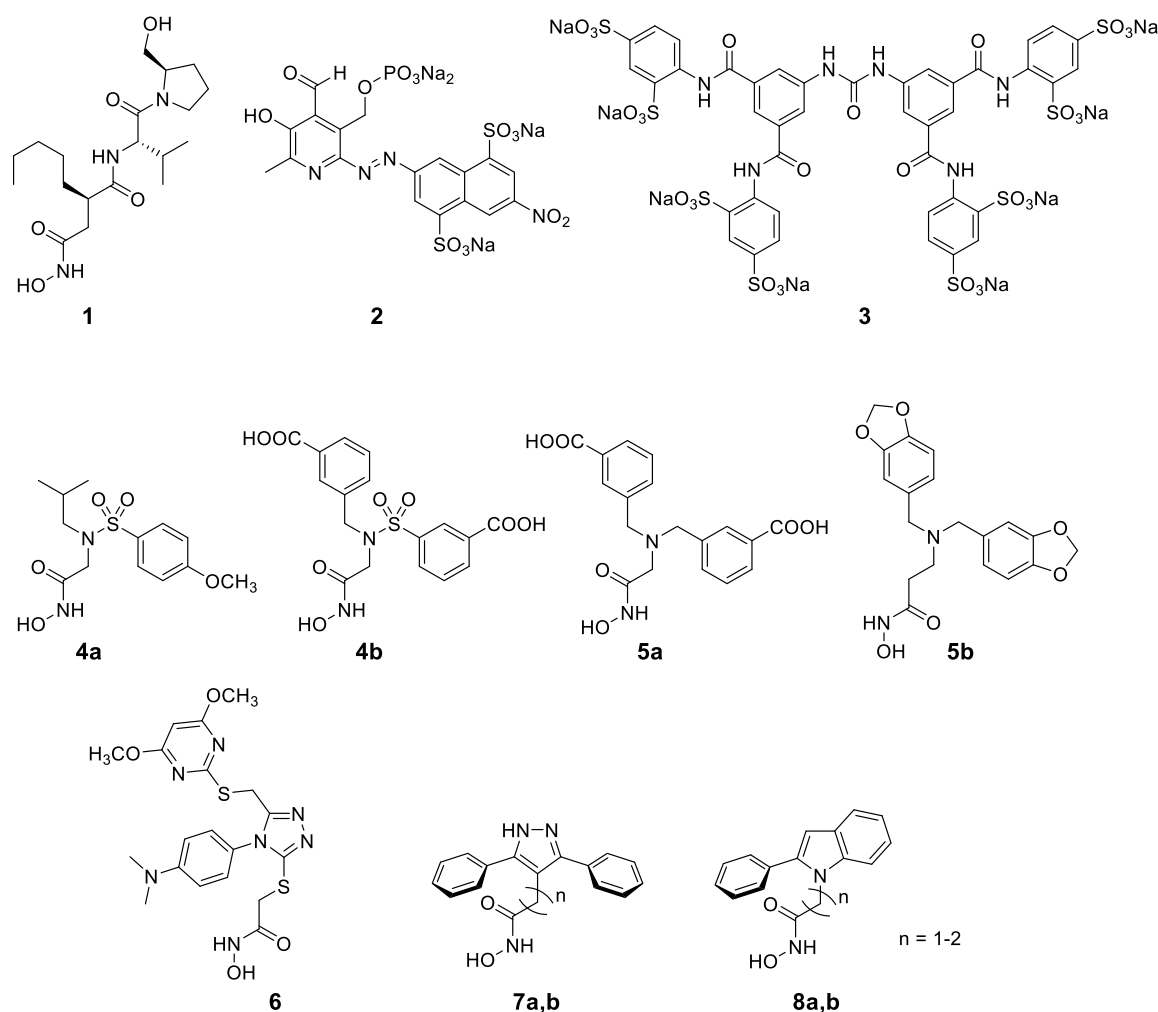


Figure 1 Examples of known inhibitors of meprin α and β

More recently, novel heteroaromatic inhibitors of meprins have been reported that were discovered by high throughput screening (**6**) or scaffold-hopping (e.g. **7a,b** & **8a,b**), respectively.³⁶⁻³⁸ The latter monocyclic or fused heteroaromatic derivatives represent the most potent inhibitors of meprins that have been reported to date, even without any functionalization of the actual diaryl-heteroaromatic scaffold.

Since they also exhibit a favorable selectivity profile over other metalloproteases, these heteroaromatic derivatives represent promising lead structures. Thus, we aimed at further optimization of this inhibitor scaffold in the present study.

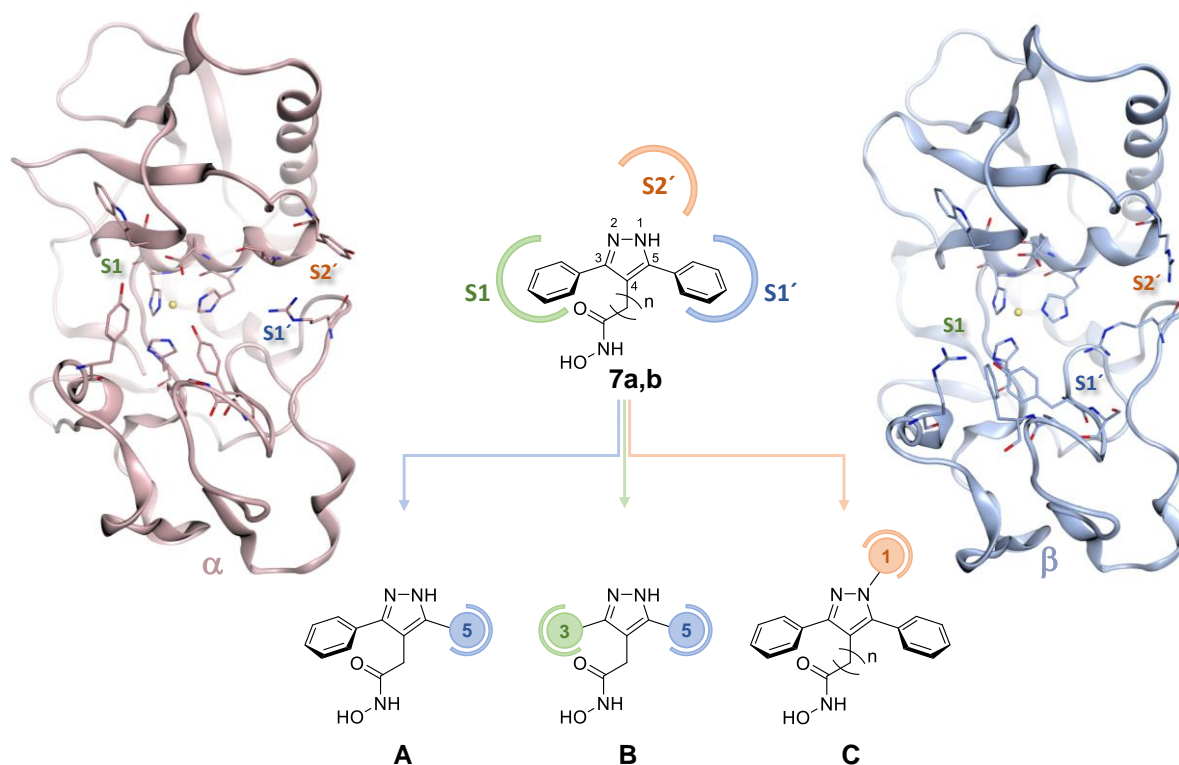


Figure 2 Protease domains of meprin α and β . Possible modifications of the pyrazole scaffold to address and modulate interactions with the S1, S1' or S2' pocket of meprin α and β are depicted

In order to modulate the inhibitory activity and selectivity between meprin α and meprin β , further derivatization of the heteroaromatic scaffold was explored. We considered the pyrazole scaffold as particularly suitable for further structural modifications, since the 3,5-diphenylpyrazole (**7a**) already exhibited high potency against meprin α . Moreover, the synthesis of pyrazole derivatives is quite established and thus enables a straightforward SAR exploration. Thus, modifications in positions 3 and 5, covering symmetric and unsymmetrical substitution, were evaluated. Based on our previous docking studies, the aryl moieties are targeting most likely the S1 and S1'-pocket of meprin α and β . Hence, the introduction of different functional groups was expected to modulate the activity against both meprins by addressing the conserved arginine residue in S1' or modulate the selectivity for either isoenzyme by interacting with the S1 site, formed by tyrosine in meprin α vs. arginine in meprin β . To address additional binding pockets, e.g. the S2'pocket, we also aimed at the introduction of *N*-substituted

pyrazoles to further modulate the activity of the inhibitors (Figure 2). Like the S1 pocket, S2' differs in both meprins as well, i.e. tyrosine in meprin α and arginine in meprin β . Hence, these modifications could also contribute to alter the selectivity profiles against the individual isoenzymes.

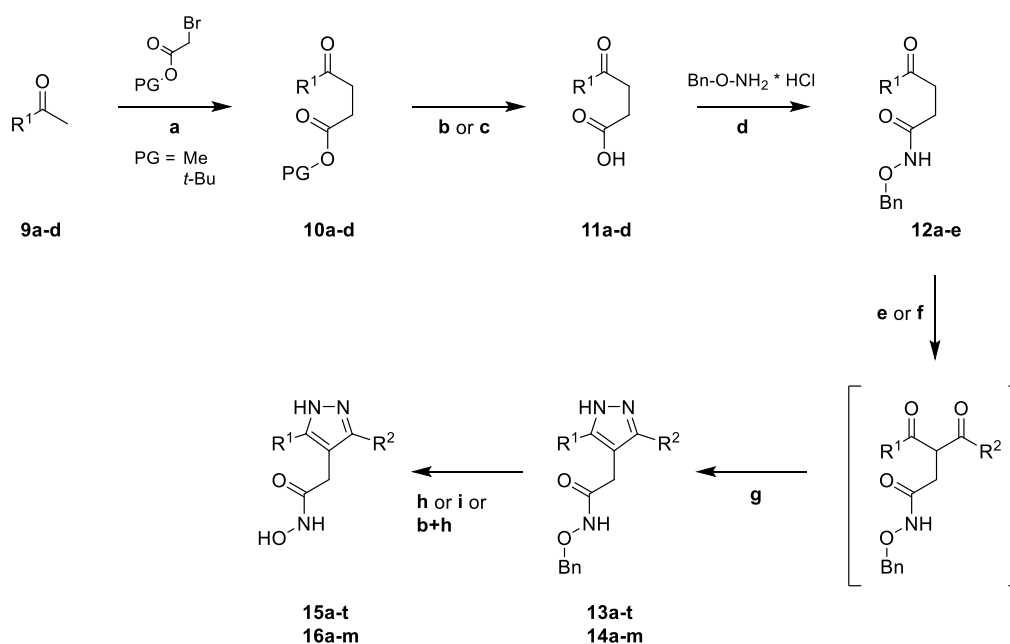
Results & Discussion

Synthesis

The 3,4,5-substituted pyrazole derivatives (**15a-t** and **16a-m**) were synthesized starting from the respective acetophenones (**9**). After alkylation with either methyl bromoacetate or *tert*-butyl bromoacetate, in accordance with orthogonal protection, the protecting group of the 3-benzoylpropionic acid ester (**10**) was cleaved by either basic or acidic conditions to yield the corresponding 3-benzoylpropionic acid (**11**). The protected hydroxamic acid was introduced by coupling of **11** with benzylhydroxylamine. The formation of the pyrazole core was accomplished using a one-pot method reported by Heller et al.³⁹ The 1,3-diketone intermediates were synthesized from the *N*-benzyloxy-4-oxo-4-phenylbutanamide derivatives (**12**) and either acid chlorides or carboxylic acids and carbonyldiimidazole. The 1,3-diketones were converted in situ into the respective pyrazoles (**13 & 14**) by subsequent addition of hydrazine monohydrate. Depending on the protecting groups, the final deprotection was carried out in different manners. The cleavage of the benzyl protecting group was accomplished by hydrogenation. Alternatively, boron tribromide enabled the concomitant cleavage of methoxy-protected groups of phenol residues, carboxylic acid esters and the benzyl-protecting group of the hydroxamic acid. Derivatives bearing an ester residue could not be treated with boron tribromide if another unstable group was present, i.e. a benzodioxolane, and were deprotected via basic hydrolysis to the corresponding carboxylic acid and hydrogenation for benzyl deprotection.

The synthesis of *N*-substituted 3,5-diphenylpyrazoles (**21a-i** and **22**) was accomplished starting from 3,5-diphenylpyrazole ester derivatives (**17 & 18**). The 3,5-diphenylpyrazole methyl esters as starting materials could be obtained by cyclocondensation of the respective 1,3-diphenylpropan-1,3-diones and hydrazine dihydrochloride (supporting information). The introduction of diverse substituents was carried out by different approaches.

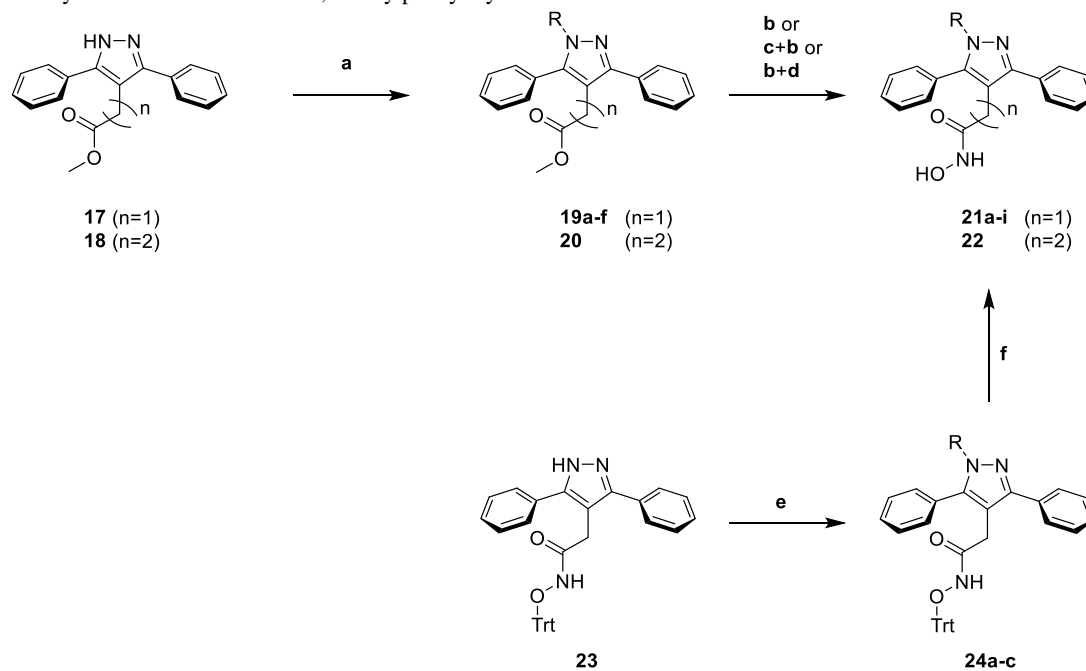
Scheme 1 Synthesis of functionalized 3,5-diarylpyrazole hydroxamic acid derivatives



Reagents and conditions: a) DMPU, LiHMDS, THF, -60 °C to rt; b) LiOH·H₂O, THF/H₂O (3:1, v/v), rt; c) TFA/DCM (1:1, v/v), rt; d) TBTU, DIPEA, DMF, rt; e) R²-COCl or acid anhydride, LiHMDS, toluene, 0 °C to rt (for **15a-f,q**, **16a,k**); f) i: R²-COOH, CDI, THF, rt, ii: LiHMDS, toluene, 0 °C to rt (for **15g-p,r-t**, **16b-j,l,m**); g) N₂H₄·H₂O, AcOH, toluene, EtOH, THF, rt to 50 °C; h) H₂, 4 bar, Pd/C, MeOH/THF (1:1, v/v), rt; i) BBr₃, DCM, 0 °C to rt

Alkyl or benzyl moieties were introduced by *N*-alkylation using sodium hydride and the respective alkyl or benzyl halides at room temperature. The *N*-substituted pyrazole ester intermediates (**19 & 20**) were converted to the respective hydroxamates by means of hydroxylamine hydrochloride under microwave irradiation. Compounds with *tert*-butyl ester groups as part of substituent R were deprotected under acidic conditions using trifluoroacetic acid in dichloromethane yielding the carboxylic acids before the conversion to the hydroxamic acid was accomplished. Pyrazole derivatives bearing a phenol residue within group R required an additional deprotection step using boron tribromide to cleave the methoxy protecting group. The introduction of *N*-aryl moieties was accomplished by Chan-Lam coupling using the corresponding phenyl boronic acid and the trityl-protected pyrazole hydroxamate with C₁ spacer (**23**). The trityl-protected analogues (**24**) were treated with trifluoroacetic acid in dichloromethane yielding the respective *N*-aryl pyrazoles (**21b-d**).

Scheme 2 Synthesis of N-substituted 3,5-diarylphenyl hydroxamic acid derivatives

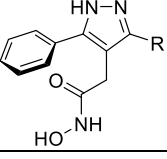
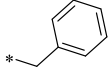
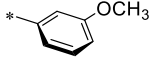
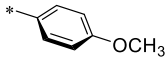
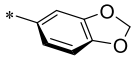
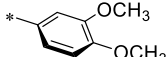
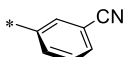
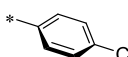
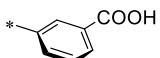
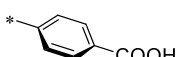
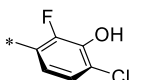
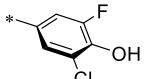
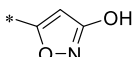
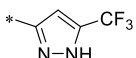
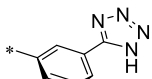


Reagents and conditions: a) i: NaH, DMF, 0 °C, ii: R-Hal, 0 °C to rt (for **21a,e-i**, **22**); b) NH₂OH·HCl, NaOCH₃, MeOH, μW, 80 °C; c) TFA/DCM (1:1, v/v), rt; d) BBr₃, DCM, 0 °C to rt; e) R-B(OH)₂, Cu(OAc)₂, TEA, MS 3Å, DCM, rt (for **21b-d**); f) TFA/DCM (1:1, v/v), TIS, rt

Structure-Activity Relationships

For exploration of the SAR, the structural variation of one moiety at position 3(5) of the 3,4,5-substituted pyrazoles was initially evaluated (Table 1). The 3,5-diphenylpyrazole **7a** without any further functionalization of the phenyl moieties already exhibited a high inhibitory activity against meprin α in the low nanomolar range. The introduction of residues with different size, i.e. methyl (**15a**) or benzyl group (**15b**) revealed a decrease in inhibitory activity, whereas the pyrazole derivative bearing a cyclopentyl moiety (**15c**) exhibited similar activities compared to **7a**. This underpins the predicted binding mode of the heteroaromatic inhibitors from previous docking studies, that suggested one phenyl substituent being orientated towards the S1'-subsite.³⁷ Thus, the lack of interactions of the methyl moiety or a different orientation by the benzyl moiety within the S1'-binding site could lead to a decrease in meprin inhibition. The introduction of a cyclic moiety, directly connected to the pyrazole core is favorable for the inhibition of meprin α and β and might address the S1'-subsite like the phenyl residue found in **7a**. Since the phenyl moiety was determined to be most favored, a series of structural modifications of the phenyl moiety was further explored and revealed inhibitory activities in the nanomolar and even picomolar range.

Table 1: Inhibition of meprin α and β by 3,4,5-substituted pyrazoles (structural variation of one aryl moiety)

	R	$K_i^{(app)}$ [nM] ^[a]		SF ^[b]
		Meprin α	Meprin β	
7a		1.3 (1.19)	115.8 (1.08)	116
15a		302.0 (1.12)	2110.8 (1.10)	7
15b		69.7 (1.05)	1733.4 (1.11)	25
15c		5.6 (1.11)	319.7 (1.06)	53
15d		1.1 (1.10)	116.0 (1.14)	105
15e		1.3 (1.14)	62.0 (1.04)	48
15f		1.1 (1.09)	109.1 (1.09)	99
15g		0.7 (1.31)	83.2 (1.05)	117
15h		4.8 (1.10)	334.7 (1.06)	67
15i		13.6 (1.04)	995.0 (1.14)	71
15j		7.5 (1.33)	47.5 (1.16)	6
15k		17.2 (1.16)	116.0 (1.15)	7
15l		2.2 (1.23)	60.6 (1.10)	31
15m		0.1 (1.62)	0.4 (1.14)	3
15n		15.9 (1.26)	13.9 (1.08)	1
15o		1.6 (1.14)	88.4 (1.12)	55
15p		0.7 (1.09)	6.7 (1.15)	10
15q		0.3 (1.35)	32.6 (1.16)	127
15r		1.4 (1.25)	54.5 (1.15)	39
15s		11.6 (1.15)	97.7 (1.09)	8
15t		9.9 (1.18)	34.9 (1.15)	4

[a] Geometric mean of three independent experiments with standard deviation factor. [b] SF: selectivity factor ($K_i^{(app)}$ meprin β / $K_i^{(app)}$ meprin α)

Electron rich moieties (**15d-15g**) were tolerated for the inhibition of meprin α and β , but electron deficient cyanoaryl moieties (**15h, 15i**) led to reduced inhibition of meprin α and β . However, the introduction of different electron rich moieties such as methoxyphenyl groups (**15d, 15e**) did not lead to a further increase in inhibitory activity compared to the unsubstituted 3,5-diphenylpyrazole **7a** and also the increase of the electron density with the introduction of a benzodioxolane (**15f**) or dimethoxyphenyl moiety (**15g**) had no major impact on the binding affinities. For pyrazole derivatives bearing acidic carboxyphenyl moieties (**15j, 15k**), an increased inhibition of meprin β in case of a *meta*-substitution could be observed. Nevertheless, the compounds still remained more active against meprin α , although the potency was slightly reduced compared to **7a**. To elaborate the influence of acidic substituents further, the introduction of carboxylic acid bioisosters (**15l-15p**) was evaluated, resulting in a general improvement of meprin β inhibition. A minor increase in the potency against meprin β could be observed for pyrazoles bearing a halogenphenol in meta-position (**15l**) and trifluoromethyl pyrazole moiety (**15o**). A further improvement in meprin β activity by factor 16 compared to **7a** could be achieved with the introduction of a phenyltetrazole moiety (**15p**), although this compound is still a more potent inhibitor of meprin α . An equipotent inhibition of both meprin isoenzymes could be observed with the halophenol (**15m**) and 3-hydroxy-isoxazol moiety (**15n**). However, the introduction of the acidic phenol in para-position (**15m**) led to strongest increase in activity against meprin α and β , respectively. Hence, this is the most potent small molecule inhibitor of both meprins so far.

The high potency of **15m** against meprin α and β , might be visualized by a respective docking pose, which revealed the interaction of the halophenol moiety within the S1'-subpocket (Figure 3). Thus, a possible interaction of the acidic moiety with the corresponding arginine residue (R²⁴² in meprin α , R²³⁸ in meprin β) via ionic interactions or charged hydrogen bonds could contribute to the potent inhibition. Moreover, π - π interactions of the pyrazole core with either Y¹⁸⁷ in meprin α , shaping the S1-subsite, or Y²¹¹ in meprin β are suggested. For meprin β , the formation of another hydrogen bond involving the phenol and S²¹² could be possible. Such a hydrogen bond network was already observed for the interaction of meprin β with compound **5a**, earlier.³³

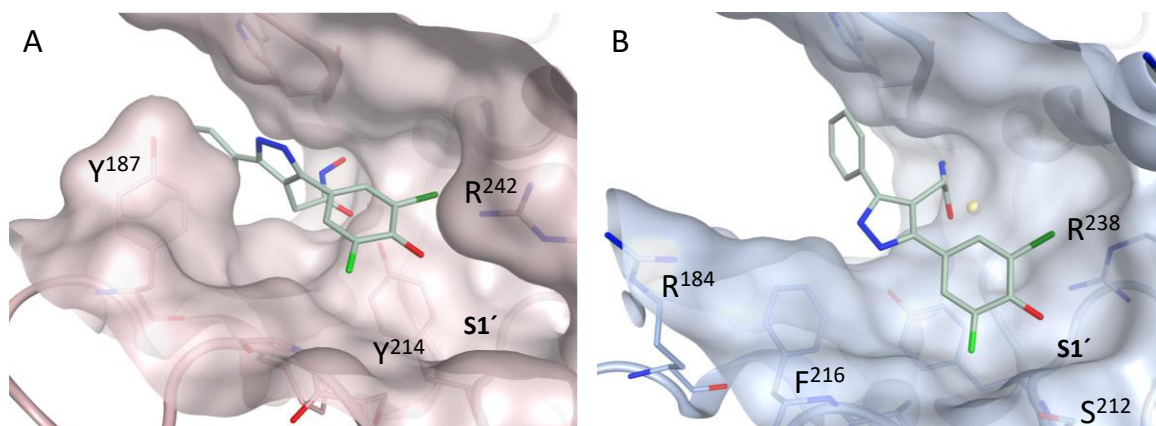


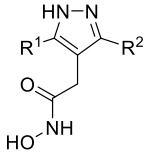
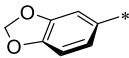
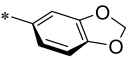
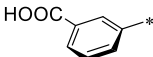
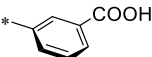
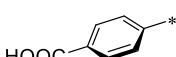
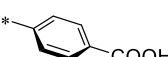
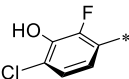
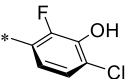
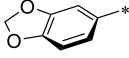
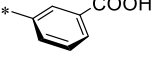
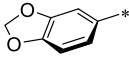
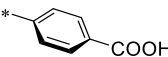
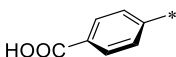
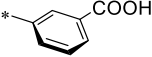
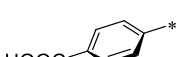
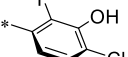
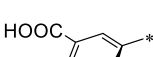
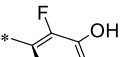
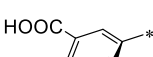
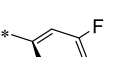
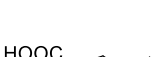
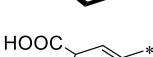
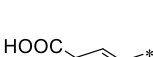
Figure 3. Putative binding mode of **15m** found by docking to the active site of meprin α (A) and meprin β (B)

Since the replacement of one phenyl moiety by an aliphatic ring was tolerated (**15c**), also cyclohexylcarboxylic acids were introduced to increase the sp^3 -content of the compounds (**15q-t**). Regardless of the substitution pattern, an increased potency against meprin β could be observed, comparable to **15j**, suggesting an interaction with arginine in either S1 or S1' pocket of meprin β . However, the activity against meprin α was less affected.

Further modification of both phenyl moieties at position 3 and 5 of the pyrazole core (Table 2, **16a-j**) indicated that the introduction of a second substituent had only a marginal impact on the inhibitory activities against meprin α and β in comparison to the monosubstituted pyrazoles (**15f,j-m**). Nevertheless, the respective compounds exhibit a further improved selectivity against off-target protease (vide infra). The introduction of two electron rich moieties (**16a**) led to an inhibitor with similar activities compared to its monosubstituted pyrazole analogue (**15f**). With the combination of an electron rich benzodioxolane moiety with an acidic carboxyphenyl moiety, i.e. compound **16e** and **16f**, a reduction of the meprin α selectivity by factor ~ 10 - 20 could be observed compared to the pyrazole bearing two benzodioxolane moieties (**16a**) underpinning the preference for acidic residues of meprin β for inhibitor binding. In order to further improve the meprin β activity and selectivity, different combinations of acidic moieties, i.e. carboxyphenyl, cyclohexylcarboxylic acid and halogenphenol moieties (**16b-d**, **16g-m**) were investigated. However, the introduction of a second acidic moiety did not lead to a noticeable difference in activity compared to the monosubstituted pyrazole analogues (**15j-m**). Hence, the

introduction of two acidic moieties did not lead to an improvement in the meprin β selectivity, but revealed equipotent inhibition of meprin α and β . This is in contrast to the structure-activity relationships of the tertiary amines, where meprin β selectivity could be obtained by the introduction of two acidic substituents that could address the S1' as well as S1-subsite.³¹

Table 2: Inhibition of meprin α and β by 3,4,5-substituted pyrazoles (structural variation of both aryl moieties)

	R ¹	R ²	K _i ^(app) [nM] ^[a]		
			Meprin α	Meprin β	SF ^[b]
16a			0.6 (1.08)	112.9 (1.12)	177
16b			9.9 (1.00)	14.5 (1.22)	1
16c			55.8 (1.03)	116.3 (1.01)	2
16d			4.2 (1.08)	13.9 (1.12)	3
16e			3.1 (1.14)	44.4 (1.04)	15
16f			10.5 (1.05)	92.8 (1.02)	9
16g			20.3 (1.02)	32.5 (1.17)	2
16h			9.6 (1.05)	11.2 (1.06)	1
16i			5.1 (1.02)	4.0 (1.51)	1
16j			0.1 (1.35)	0.2 (1.13)	2
16k			0.4 (1.21)	5.2 (1.16)	13
16l			19.8 (1.10)	20.9 (1.16)	1
16m			21.0 (1.14)	14.5 (1.08)	0.7

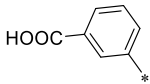
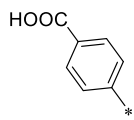
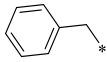
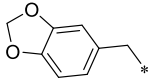
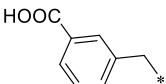
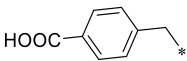
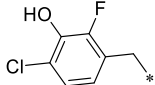
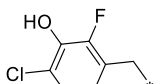
[a] Geometric mean of three independent experiments with standard deviation factor; [b] SF: selectivity factor ($K_i^{(app)}$ meprin β / $K_i^{(app)}$ meprin α)

The pyrazole core was found by a scaffold hopping approach in order to rigidify the tertiary amine scaffold.³⁸ Although this was successful and led to a series of highly potent heteroaromatic inhibitors of meprins, in particular against meprin α , these compounds obviously lack a certain degree of flexibility or less suitable binding of the scaffold that is required to achieve meprin β selectivity. The latter seems to be mainly driven by addressing arginine residues in S1 and S1' by ionic interactions of the tertiary amine derived inhibitors. Due to the relatively rigid body of the diphenyl pyrazole core, the acidic moieties cannot be placed in a right position to form the required ionic interactions with both arginine residues in S1 and S1', respectively. Hence, despite their high potency, a high selectivity for meprin β as found for the tertiary amines could not be achieved by the investigated compounds.

In addition to the evaluation of the structural modifications at position 3 and 5 of the pyrazole, the influence of the *N*-substitution on the binding affinity was elaborated (**Fehler! Verweisquelle konnte nicht gefunden werden.** and 4). The *N*-substitution was performed from 3,5-diphenylpyrazole **7a**. The introduction of different lipophilic moieties, i.e. methyl (**21a**) and phenyl moiety (**21b**), resulted in a 4 to 6-fold decrease in activity against meprin α and β compared to the unsubstituted 3,5-diphenylpyrazole **7a**. However, the extension of the pyrazole with a benzyl moiety (**21e**) demonstrated no significant reduction of the inhibitory activities, although meprin β activity is slightly decreased in comparison to **7a**. Further variation of the *N*-phenyl pyrazole by the introduction of acidic carboxyphenyl residues (**21c**, **21d**) led to an increased inhibition of meprin β by factor 3 in comparison to the *N*-phenyl pyrazole **21b**. This also corroborates the preference of acidic moieties at this position, in particular for meprin β with an additional arginine in S2', i.e. R¹⁴⁶.

Since the introduction of a benzyl moiety at position 1 of the pyrazole (**21e**) was well tolerated, we assumed that this moiety could be explored for further modifications. The introduction of an electron-rich benzodioxolane moiety (**21f**), that additionally could serve as hydrogen bond acceptor, had only a marginal effect on the inhibitory activity against meprin α compared to the *N*-benzylated pyrazole **21e**. In contrast to that, introduction of acidic moieties had a greater impact on the inhibitory activities.

Table 3 Inhibition of meprin α and β by N-substituted 3,5-diphenylpyrazoles

		R	n	$K_i^{(app)}$ [nM] ^[a]		SF ^[b]
				Meprin α	Meprin β	
7a		H _*	1	1 (1.19)	116 (1.08)	116
21a		H ₃ C _*	1	5 (1.02)	437 (1.08)	87
21b			1	4 (1.04)	667 (1.09)	167
21c			1	4 (1.08)	212 (1.06)	53
21d			1	4 (1.12)	182 (1.09)	46
21e			1	1 (1.08)	291 (1.12)	291
21f			1	0.6 (1.23)	305.0 (1.02)	508
21g			1	0.3 (1.12)	10.6 (1.14)	35
21h			1	0.4 (1.36)	9.4 (1.16)	24
21i			1	0.08 (1.30)	9.3 (1.04)	116
22			2	0.15 (1.26)	1183.8 (1.09)	7892

[a] Geometric mean of three independent experiments with standard deviation factor; [b] SF: selectivity factor ($K_i^{(app)}$ meprin β / $K_i^{(app)}$ meprin α)

The aromatic carboxylic acid substitutions at a benzylic unit (**21g, h**) resulted in a 3-fold improved activity against meprin α and had even a particularly favorable effect on the inhibition of meprin β with a 30-fold increase in potency compared to **21e**. This also affected the selectivity of meprin α , which shifted from a three-digit to a two-digit range. The replacement with a bioisosteric halophenol moiety

(**21i**) led to a comparable improvement of the potency against meprin β in the lower nanomolar range. However, the halophenol moiety of **21i**, with hydroxyl function in *meta*-position, was much more preferred for the inhibition of meprin α compared to **21g** or **h** and exhibited an increased inhibitory activity in the picomolar range. Our recent study has shown that the extension of the spacer length of the hydroxamic moieties to the heteroaromatic core led to a reduction of the inhibitory activity against meprin α and β , but slightly increased the selectivity for meprin α .³⁸ Similarly, for compound **22** the extension of the spacer length from C1 to C2 spacer was again less favored for the inhibition of meprins. However, while the activity against meprin α was virtually not affected, the $K_i^{(app)}$ value against meprin β declined by a factor ~ 120 compared to **21i** and thereby led to an exceptional high selectivity of meprin α over meprin β with a factor of almost 7900.

To obtain a better understanding for the consistently high potency of compound **22** against meprin α , despite the variation of the spacer length, docking studies of **21i** with C1 spacer and **22** with C2 spacer were performed (Figure 4).

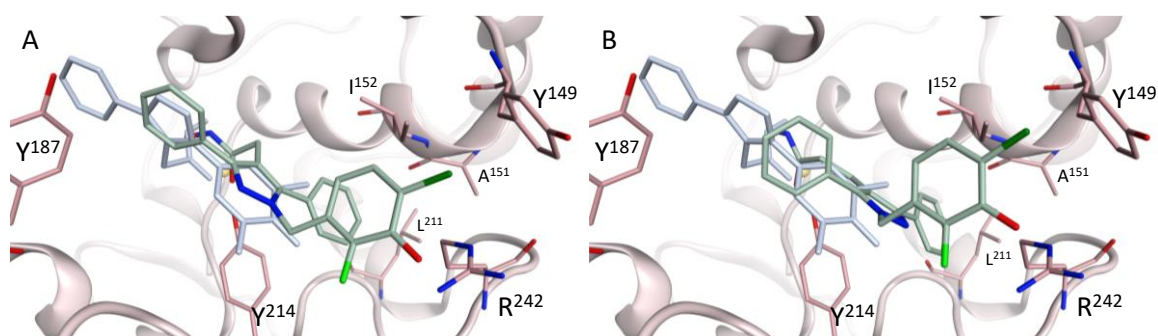


Figure 4: Docking solutions of **21i** (A) and **22** (B) to the active site of meprin α in comparison to **15m** (light blue)

The resulting docking solutions revealed binding poses of the *N*-substituted diphenylpyrazole **21i** and **22** that differ from the predicted binding mode of the docked 3,4,5-substituted pyrazole **15m** in meprin α . While the docking solution of **15m** involves π - π interactions of the pyrazole core with Y¹⁸⁷ in the S1-subpocket, the *N*-substituted pyrazole **21i** and **22** is moved away from the S1-subsite. Regardless of the spacer length, the halophenol moiety of both, **21i** and **22**, could address the S1'-subsite via an ionic interaction or charged hydrogen bond to arginine residue R²⁴². Moreover, this predicted shift of the binding mode enables one phenyl moiety to interact with an additional lipophilic subpocket,

shaped by I¹⁵², A¹⁵¹ and L²¹¹, thus further increasing the binding affinity via hydrophobic contacts. Based on the docking solutions, this interaction might be more favored in case of **22**, since the longer spacer allows the ligand to plunge deeper in this pocket. The positioning of the pyrazole derivative **21i** with C1 spacer could also enable π - π interactions of Y¹⁸⁷ and the phenyl moiety. However, the extension of the spacer length leads to a slightly different positioning of the diphenylpyrazole **22** with C2 spacer within the active site compared to the shorter analogue **21i**, thus ruling out potential π - π interactions with Y¹⁸⁷. However, according to the predicted binding mode, both inhibitors are able to form a Cl- π interaction⁴¹. This interaction involving the halophenol moiety and Y¹⁴⁹ in S2' of meprin α would contribute to the activity against meprin α and also to the selectivity against meprin β . In meprin β , S2' is formed by an arginine residue, thus ruling out the respective interaction to the halogen of the inhibitor. Additionally, the extension of the spacer from C1 to C2 enhances the selectivity, most likely due to steric reasons. However, the exceptional high selectivity of **22**, i.e. factor 7900, cannot be deduced from the obtained docking results.

Selectivity profile and *in vitro* toxicity

The evaluation of the heteroaromatic inhibitors already revealed a favorable selectivity profile over the inhibition of selected off-target metalloproteases.³⁸ With the structural variation of the 3,5-diphenylpyrazole (**7a**) further studies of selected derivatives for possible alterations in off-target selectivity were performed (**Fehler! Verweisquelle konnte nicht gefunden werden.**). The introduction of several substituents at position 3(5) (**15d**, **15f**, **15g**, **15m**) led to minor alterations in the inhibition of MMP and ADAM proteases compared to **7a**. The off-target selectivity was more affected by the structural modification of the second aryl moiety, as a pyrazole bearing two benzodioxolane moieties (**16a**) exhibited a higher inhibition of the related metalloproteases, particularly MMP2 with a residual activity of 29% at 10 μ M inhibitor concentration. By contrast, the introduction of two acidic moieties (**16j**) abolished the inhibition of the respective MMPs and ADAMs that led to an excellent high selectivity with residual activities above 90%. While the modification of both aryl residues at position 3 and 5 did not lead to any differences in the inhibitory activity against meprin α and β , an impact on the inhibition of the off-target metalloproteases could be observed, leading to decreased inhibition even

at higher concentrations (not shown). The evaluation of selected *N*-substituted pyrazoles (**21f-i**, **22**) revealed residual activities that are mostly comparable to **7a**, with inhibition less than 50% at a concentration of 10 μ M, except a stronger inhibition of MMP2 by **21f**. However, the slightly increased inhibition of individual off-target proteases by a few pyrazole derivatives, i.e. **15d,f & 16a, 21f**, corresponds to IC₅₀-values in the μ M-range (table 5). Thus, the compounds still exhibit high selectivity for meprin α with a selectivity of three orders of magnitude compared to the K_i^(app) values in the low nanomolar and upper picomolar range. In addition, the cell viability of liver and neuronal cell lines was determined for selected compounds, proving no *in vitro* toxicity of the tested compounds.

Table 4: Inhibition of off-target metalloproteases by selected 3,4,5-substituted pyrazole inhibitors

	Residual activity [%] ^[a]					Cell viability [%] ^[b]	
	MMP2	MMP9	MMP13	ADAM10	ADAM17	Hep-G2	SY5Y
7a	104	81	75	73	61	100	92
15d	78	80	85	68	52	104	84
15f	41	72	71	59	51	96	90
15g	83	90	101	87	65	99	85
15m	66	86	88	104	68	103	86
16a	29	63	56	62	57	n.d.	n.d.
16j	95	94	105	90	99	98	110
21f	77	74	78	69	21	103	88
21g	89	83	83	92	84	99	85
21h	85	80	86	91	67	103	88
21i	69	70	84	85	72	107	79
22	102	100	98	117	90	100	98

[a] Residual activity [%] @ 10 μ M inhibitor concentration
[b] Inhibitor concentration 30 μ M
n.d. – not determined

Table 5: Inhibitory activities against MMP2, MMP13, ADAM10, ADAM17 of selected compounds

IC ₅₀ [μ M] ^[a]	MMP2	MMP13	ADAM10	ADAM17
15d	n.d.	n.d.	n.d.	11.6 (1.05)
15f	5.3 (1.11)	n.d.	13.9 (1.00)	7.4 (1.10)
16a	1.4 (1.34)	15.7 (1.53)	12.0 (1.02)	9.6 (1.06)
21f	n.d.	n.d.	n.d.	2.3 (1.22)

[a] IC₅₀ [μ M] as geometric mean with standard deviation factor

Conclusion

Based on emerging roles of meprin α and β in the pathophysiology of various diseases, the inhibition of these astacin proteases could provide novel therapeutic opportunities. Highly potent and selective inhibitors are needed to further assess the therapeutic relevance of the potential targets in target validation experiments. Recently, the discovery of novel heteroaromatic scaffolds for the development of astacin protease inhibitors resulted in a significantly improved inhibitory activity, in particular with respect to the inhibition of meprin α . Demonstrating a favorable off-target selectivity and no *in vitro* cytotoxicity, the heteroaromatic cores were identified as potential lead structures. Therefore, further modifications of the pyrazole scaffold were evaluated. Within this study different structural modifications at position 1, 3 and 5 of the pyrazole core were explored, yielding novel meprin inhibitors that exhibit high inhibitory activities down to the picomolar range. Structural variations of the substituents enabled the modulation of the selectivity within the meprin isoforms for some compounds that lead to either equipotent meprin α and β inhibitors or a few highly potent meprin α inhibitors with excellent selectivity over meprin β . In particular, the remarkable off-target selectivity against related metalloproteases and lacking *in vitro* toxicity of the novel pyrazole derivatives allows the application of these compounds as chemical probes for target validation to further assess the functional roles of meprin proteases, in particular meprin α in the disease progression.

Experimental section

Chemistry

General. Starting materials and solvents were purchased from Aldrich, Activate Scientific, Alfa Aesar, Iris Biotech and Merck Millipore. The purity of the compounds was assessed by HPLC and confirmed to be $\geq 95\%$. The analytical HPLC-system consisted of a Merck–Hitachi device (model LaChrom) utilizing a Phenomenex Luna 5 μM C18(2) column (125 mm \times 4.0 mm) with $\lambda = 214$ nm as the reporting wavelength. The compounds were analyzed using a gradient at a flow rate of 1 mL/min, whereby eluent (A) was acetonitrile, eluent (B) was water, both containing 0.04% (v/v) trifluoro acetic acid applying the following gradient: 0 min – 15 min: 5–60% (A), 15 min – 20 min: 60–95% (A), 20–30 min: 95%

(A), 30–31 min: 95–5% (A), 31–35 min: 5% (A). The purities of all reported compounds were determined by the percentage of the peak area at 214 nm. ESI-Mass spectra were obtained with an Expression CMS spectrometer (Advion). The high-resolution positive ion ESI mass spectra were obtained from a LTQ Orbitrap XL (Thermo Fisher Scientific). The ¹H NMR spectra were recorded at a Bruker Avance III 400 MHz and 700 MHz. DMSO-d₆ was used as solvent unless otherwise specified. Chemical shifts are expressed as parts per million (ppm). The solvent was used as internal standard. Splitting patterns have been designated as follows: s (singlet), d (doublet), dd (doublet of doublet), t (triplet), m (multiplet), and br (broad signal). Semipreparative HPLC was performed on a Prepstar device (Varian) equipped with a Phenomenex Luna 10 μM C18(2) column (250 mm × 21 mm). The compounds were eluted using the same solvent system as described above, applying a flow rate of 21 mL/min.

General Method for the synthesis of 3-benzoylpropionic acid ester derivatives 10a-d

The respective acetophenone derivative (1 equiv) was dissolved in dry toluene (c=1 M). After the solution was cooled to –60 °C, DMPU (3.6 equiv) and LiHMDS (1 M in THF, 1.2 equiv) were added via syringe under argon atmosphere. After 30 minutes of stirring, methyl bromoacetate or *tert*-butyl bromoacetate (1.5 equiv) was added dropwise. The mixture was stirred for an additional 10 minutes, then allowed to warm up to room temperature and stirred for further 5 hours. The volatiles were evaporated and the remains were taken up with a small amount of water. The aqueous layer was slightly acidified by means of diluted aqueous HCl and was extracted with EtOAc (3x25 ml). The combined organic layers were dried over Na₂SO₄ and evaporated. The residue was purified by flash chromatography (silica, heptane/diethyl ether or heptane/EtOAc gradient)

General method for the synthesis of 3-benzoylpropionic acids 11a-d

Method A: The respective methyl ester derivative was dissolved in THF/water (3:1 v/v, c=0.4 M). LiOH·H₂O (2 equiv) was added and the mixture was stirred overnight at room temperature. The volatiles were evaporated and the remains were taken up in water, acidified by means of diluted aqueous HCl and extracted with EtOAc (3x25 ml). The combined organic layers were dried over Na₂SO₄ and evaporated. The residue was used without further purification.

Method B: The respective *tert*-butylester derivative was treated with TFA/DCM (1:1 v/v, 10 ml) at 0 °C and stirred for 2-4 hours. The volatiles were evaporated, and the remains were purified by flash chromatography (silica, heptane/EtOAc gradient).

General method for the synthesis of *O*-benzyl hydroxamic acid derivatives 12a-e

The respective 3-benzoylpropionic acid (1 equiv) was dissolved in DMF (c=0.5 M). TBTU (1 equiv) and DIPEA (1 equiv) were added to the solution and the mixture was stirred at room temperature for several minutes. Subsequently *O*-benzylhydroxylamine hydrochloride (1 equiv) and DIPEA (3.2-4 equiv) were added and the mixture was stirred at room temperature for another 3 hours. The reaction was quenched with water and extracted with EtOAc (3x25 ml). The combined organic layers were dried over Na₂SO₄ and evaporated. The residue was purified by flash chromatography (silica, heptane/EtOAc gradient).

General method for the synthesis of 3,4,5-substituted pyrazole derivatives 13a-t, 14a-m

Method A: The respective *N*-benzyloxy-4-oxo-4-phenylbutanamide derivative (1 equiv) was dissolved in dry toluene (c=0.4 M) in a flask sealed with a septum. The solution was cooled to 0 °C under argon. LiHMDS (1 M in THF, 2.1 equiv) was added quickly via syringe and the mixture was stirred for 5 minutes. The respective acyl chloride derivative (0.5 eq) was added in one portion and the mixture was allowed to warm up to room temperature. The mixture was stirred vigorously until TLC showed full conversion of the acyl chloride. AcOH (2 ml) was added to the mixture. EtOH (10 ml) and THF (5 ml) were added to form a homogeneous mixture, then N₂H₄*H₂O (34.3 equiv) was added. The mixture was heated to 50 °C and the reaction was monitored via TLC. The volatiles were evaporated and the remains were taken up in water, acidified by means of diluted aqueous HCl and extracted with EtOAc (3x25 ml). The combined organic layers were dried over Na₂SO₄ and evaporated. The residue was purified by flash chromatography (silica, CHCl₃/MeOH gradient).

Method B: The respective carboxylic acid derivative (0.5 equiv) was dissolved in dry THF (c=0.3 M). Under argon atmosphere CDI was added to the solution. The mixture was stirred for 1 hour at room temperature. In a separate flask the respective *N*-benzyloxy-4-oxo-4-phenylbutanamide derivative

(1 equiv) was dissolved in dry toluene ($c=0.4$ M) and sealed with a septum. The solution was cooled to 0 °C under argon. LiHMDS (1 M in THF, 2.1 equiv) was added quickly via syringe and the mixture was stirred for 5 minutes. The respective activated carboxylic acid derivative (0.5 equiv) was added in one portion and the mixture was allowed to warm up to room temperature. The mixture was stirred vigorously until TLC showed full conversion of the carboxylic acid derivative. AcOH (2 ml) was added to the mixture. EtOH (10 ml) and THF (5 ml) were added to form a homogeneous mixture, then $N_2H_4 \cdot H_2O$ (34.3 equiv) was added. The mixture was heated to 50 °C and the reaction was monitored via TLC. The volatiles were evaporated and the remains were taken up in water, acidified by means of diluted aqueous HCl and extracted with EtOAc (3x25 ml). The combined organic layers were dried over Na_2SO_4 and evaporated. The residue was purified by flash chromatography (silica, $CHCl_3/MeOH$ gradient).

General methods for deprotection of hydroxamic acid derivatives 15a-t, 16a-m

Method A: The respective benzyl-protected hydroxamic acid was dissolved in DCM (5 ml) in a sealed flask under argon atmosphere. The mixture was cooled down to 0 °C and treated with BBr_3 (1 M in DCM, 3-19 equiv). The mixture was allowed to warm up to room temperature and was stirred overnight. The reaction was quenched with water and cooled with ice. The aqueous phase was extracted with EtOAc (3x25 ml). The combined organic layers were dried over Na_2SO_4 and evaporated. The residue was purified by semi-preparative HPLC.

Method B: The respective ester derivative was dissolved in a mixture of THF/ H_2O (3:1 v/v, $c=0.4$ M) and was treated with lithium hydroxide monohydrate (2 equiv). The mixture was stirred overnight at room temperature. The solvent was evaporated and the remains were taken up in water, acidified by means of diluted aqueous HCl and extracted with EtOAc (3x25 ml). The combined organic layers were dried over Na_2SO_4 and evaporated. The residue was used without further purification.

Method C: The respective benzyl-protected hydroxamic acid was dissolved in a mixture of MeOH/THF (1:1 v/v, 10 ml) and treated with Pd/C (10%, 0.05 equiv). The vial was purged with hydrogen and the mixture was hydrogenated (H_2 , 4 bar) for 4-5 hours. The mixture was filtered through celite and evaporated under vacuum. The residue was purified by semi-preparative HPLC.

2-(3-Methyl-5-phenyl-1H-pyrazol-4-yl)ethanehydroxamic acid (15a)

The compound was synthesized from *N*-benzyloxy-2-(3-methyl-5-phenyl-1H-pyrazol-4-yl)acetamide (112 mg, 0.35 mmol) and BBr₃ (1 M in DCM, 697 μ l, 0.7 mmol) according to method A as described above. Yield: 22 mg (27%); ESI-MS *m/z*: 232.2 [M+H]⁺; HPLC: *rt* 6.56 min (>99%); ¹H NMR (400 MHz, DMSO-d₆): δ 2.20 (s, 3H), 3.21 (s, 1.9H), 3.55 (br s, 0.1H), 7.34-7.38 (m, 1H), 7.44 (t, 2H, ³J=7.3 Hz), 7.65-7.67 (m, 2H), 10.58 (br s, 1H) mixture of *cis-trans* isomers; HRMS *m/z*: 232.1076 [M+H]⁺; calcd for C₁₂H₁₄N₃O₂⁺: 232.1081.

2-(3-Benzyl-5-phenyl-1H-pyrazol-4-yl)ethanehydroxamic acid (15b)

The compound was synthesized from *N*-benzyloxy-2-(3-benzyl-5-phenyl-1H-pyrazol-4-yl)acetamide (102 mg, 0.26 mmol) and BBr₃ (1 M in DCM, 770 μ l, 0.77 mmol) according to method A as described above. Yield: 24 mg (30%); ESI-MS *m/z*: 308.3 [M+H]⁺; HPLC: *rt* 10.43 min (>99%); ¹H NMR (400 MHz, DMSO-d₆): δ 3.21 (s, 1.8H), 3.54 (br s, 0.2H), 3.96 (s, 2H), 7.17-7.22 (m, 1H), 7.26-7.29 (m, 4H), 7.34-7.37 (m, 1H), 7.43 (t, 2H, ³J=7.6 Hz), 7.66-7.68 (m, 2H), 9.98 (br s, 0.1H), 10.61 (br s, 0.9H) mixture of *cis-trans* isomers; HRMS *m/z*: 308.1389 [M+H]⁺; calcd for C₁₈H₁₈N₃O₂⁺: 308.1394.

2-(3-Cyclopentyl-5-phenyl-1H-pyrazol-4-yl)ethanehydroxamic acid (15c)

The compound was synthesized from *N*-benzyloxy-2-(3-cyclopentyl-5-phenyl-1H-pyrazol-4-yl)acetamide (205 mg, 0.55 mmol) and BBr₃ (1 M in DCM, 1.6 ml, 1.64 mmol) according to method A as described above. Yield: 49 mg (31%); ESI-MS *m/z*: 286.2 [M+H]⁺; HPLC: *rt* 9.07 min (>99%); ¹H NMR (400 MHz, DMSO-d₆): δ 1.60-1.71 (m, 4H), 1.74-1.78 (m, 2H), 1.93-2.00 (m, 2H), 3.05-3.13 (m, 1H), 3.22 (s, 1.9H), 3.56 (br s, 0.1H), 7.34-7.38 (m, 1H), 7.43 (t, 2H, ³J=7.3 Hz), 7.67 (d, 2H, ³J = 7.3 Hz), 9.96 (br s, 0.1H), 10.56 (br s, 0.9H) mixture of *cis-trans* isomers; HRMS *m/z*: 286.1545 [M+H]⁺; calcd for C₁₆H₂₀N₃O₂⁺: 286.1550.

2-[3-(3-Methoxyphenyl)-5-phenyl-1H-pyrazol-4-yl]ethanehydroxamic acid (15d)

The compound was synthesized from *N*-benzyloxy-2-[3-(3-methoxyphenyl)-5-phenyl-1H-pyrazol-4-yl]acetamide (226 mg, 0.55 mmol) and Pd/C (30 mg, 0.03 mmol) according to method C as described

above. Yield: 145 mg (82%); ESI-MS m/z : 324.3 $[M+H]^+$; HPLC: rt 10.69 min (97.9%); 1H NMR (400 MHz, DMSO- d_6): δ 3.32 (s, 1.8H), 3.63 (br s, 0.2H), 3.81 (s, 3H), 6.95-6.98 (m, 1H), 7.20-7.22 (m, 2H), 7.36-7.42 (m, 2H), 7.47 (t, 2H, $^3J=7.5$ Hz), 7.64-7.65 (m, 2H), 10.12 (br s, 0.1H), 10.63 (s, 0.9H) mixture of *cis-trans* isomers; HRMS m/z : 324.1341 $[M+H]^+$; calcd for $C_{18}H_{18}N_3O_3^+$: 324.1343.

2-[3-(4-Methoxyphenyl)-5-phenyl-1H-pyrazol-4-yl]ethanehydroxamic acid (15e)

The compound was synthesized from *N*-benzyloxy-2-[3-(4-methoxyphenyl)-5-phenyl-1H-pyrazol-4-yl]acetamide (305 mg, 0.74 mmol) and Pd/C (40 mg, 0.04 mmol) according to method C as described above. Yield: 114 mg (48%); ESI-MS m/z : 324.3 $[M+H]^+$; HPLC: rt 10.37 min (97.8%); 1H NMR (400 MHz, DMSO- d_6): δ 3.29 (s, 1.8H), 3.60 (s, 0.2H), 3.81 (s, 3H), 7.03 (d, 2H, $^3J=8.7$ Hz), 7.37-7.41 (m, 1H), 7.46 (t, 2H, $^3J=7.6$ Hz), 7.57 (d, 2H, $^3J=8.7$ Hz), 7.63-7.65 (m, 2H), 10.08 (br, 0.1H), 10.60 (s, 0.9H) mixture of *cis-trans* isomers; HRMS m/z : 324.1340 $[M+H]^+$; calcd for $C_{18}H_{18}N_3O_3^+$: 324.1343.

2-[3-(1,3-Benzodioxol-5-yl)-5-phenyl-1H-pyrazol-4-yl]ethanehydroxamic acid (15f)

The compound was synthesized from 2-[3-(1,3-Benzodioxol-5-yl)-5-phenyl-1H-pyrazol-4-yl]-*N*-benzyloxy-acetamide (139 mg, 0.33 mmol) and Pd/C (17 mg, 0.02 mmol) according to method C as described above. Yield: 45 mg (41%); ESI-MS m/z : 338.2 $[M+H]^+$; HPLC: rt 10.40 min (98.1%); 1H NMR (400 MHz, DMSO- d_6): δ 3.29 (s, 1.8H), 3.59 (s, 0.2H), 6.08 (s, 2H), 7.00-7.02 (m, 1H), 7.11-7.14 (m, 1H), 7.20-7.21 (m, 1H), 7.37-7.41 (m, 1H), 7.47 (t, 2H, $^3J=7.6$ Hz), 7.61-7.63 (m, 2H), 10.11 (br s, 0.1H), 10.62 (s, 0.9H) mixture of *cis-trans* isomers; HRMS m/z : 338.1133 $[M+H]^+$; calcd for $C_{18}H_{16}N_3O_4^+$: 338.1135.

2-[3-(3,4-Dimethoxyphenyl)-5-phenyl-1H-pyrazol-4-yl]ethanehydroxamic acid (15g)

The compound was synthesized from *N*-benzyloxy-2-[3-(3,4-dimethoxyphenyl)-5-phenyl-1H-pyrazol-4-yl]acetamide (120 mg, 0.27 mmol) and Pd/C (14 mg, 0.01 mmol) according to method C as described above. Yield: 49 mg (52%); ESI-MS m/z : 354.3 $[M+H]^+$; HPLC: rt 9.95 min (98.6%); 1H NMR (400 MHz, DMSO- d_6): δ 3.30 (s, 1.8H), 3.61 (br s, 0.2H), 3.80-3.81 (m, 6H), 7.03-7.06 (m, 1H), 7.15-7.17 (m, 1H), 7.23-7.24 (m, 1H), 7.37-7.41 (m, 1H), 7.47 (t, 2H, $^3J=7.6$ Hz), 7.66 (d, 2H, $^3J=7.6$ Hz),

10.13 (br s, 0.1H), 10.63 (s, 0.9H) mixture of *cis-trans* isomers; HRMS m/z: 354.1444 [M+H]⁺; calcd for C₁₉H₂₀N₃O₄⁺: 354.1448.

2-[3-(3-Cyanophenyl)-5-phenyl-1H-pyrazol-4-yl]ethanehydroxamic acid (15h)

The compound was synthesized from *N*-benzyloxy-2-[3-(3-cyanophenyl)-5-phenyl-1H-pyrazol-4-yl]acetamide (83 mg, 0.20 mmol) and BBr₃ (1 M in DCM, 610 μl, 0.61 mmol) according to method A as described above. Yield: 25 mg (39%); ESI-MS m/z: 319.2 [M+H]⁺; HPLC: rt 10.48 min (95.6%); ¹H NMR (400 MHz, DMSO-d₆): δ 3.36 (s, 1.8H), 3.66 (br s, 0.2H), 7.42-7.45 (m, 1H), 7.50 (t, 2H, ³J=7.6 Hz), 7.61-7.64 (m, 2H), 7.66-7.71 (m, 1H), 7.86 (d, 1H, ³J=7.7 Hz), 8.02 (d, 1H, ³J=7.8 Hz), 8.12 (s, 1H), 10.69 (s, 0.9H), 10.92 (s, 0.1H) mixture of *cis-trans* isomers; HRMS m/z: 319.1186 [M+H]⁺; calcd for C₁₈H₁₅N₄O₂⁺: 319.1190.

2-[3-(4-Cyanophenyl)-5-phenyl-1H-pyrazol-4-yl]ethanehydroxamic acid (15i)

The compound was synthesized from *N*-benzyloxy-2-[3-(4-cyanophenyl)-5-phenyl-1H-pyrazol-4-yl]acetamide (84 mg, 0.21 mmol) and BBr₃ (1 M in DCM, 617 μl, 0.62 mmol) according to method A as described above. Yield: 27 mg (42%); ESI-MS m/z: 319.2 [M+H]⁺; HPLC: rt 10.56 min (>99%); ¹H NMR (400 MHz, DMSO-d₆): δ 3.36 (s, 1.8H), 3.67 (br s, 0.2H), 7.42-7.45 (m, 1H), 7.50 (t, 2H, ³J=7.6 Hz), 7.62 (d, 2H, ³J=7.7 Hz), 7.88-7.94 (m, 4H), 10.15 (br s, 0.1H), 10.68 (s, 0.9H) mixture of *cis-trans* isomers; HRMS m/z: 319.1185 [M+H]⁺; calcd for C₁₈H₁₅N₄O₂⁺: 319.1190.

3-[4-[2-(Hydroxyamino)-2-oxo-ethyl]-5-phenyl-1H-pyrazol-3-yl]benzoic acid (15j)

The compound was synthesized from methyl-3-[4-[2-(benzyloxyamino)-2-oxo-ethyl]-5-phenyl-1H-pyrazol-3-yl]benzoate (117 mg, 0.27 mmol) and BBr₃ (1 M in DCM, 2.7 ml, 2.66 mmol) according to method A as described above. Yield: 5 mg (6%); ESI-MS m/z: 338.2 [M+H]⁺; HPLC: rt 9.39 min (95.8%); ¹H NMR (400 MHz, DMSO-d₆): δ 3.35 (s, 1.7H), 3.65 (br s, 0.3H), 7.40-7.43 (m, 1H), 7.49 (t, 2H, ³J=7.6 Hz), 7.57-7.65 (m, 3H), 7.89 (d, 1H, ³J=7.8 Hz), 7.96 (d, 1H, ³J=7.8 Hz), 8.27 (s, 1H), 10.12 (br s, 0.1H), 10.61 (s, 0.9H) mixture of *cis-trans* isomers; HRMS m/z: 338.1134 [M+H]⁺; calcd for C₁₈H₁₆N₃O₄⁺: 338.1135.

4-[4-[2-(Hydroxyamino)-2-oxo-ethyl]-5-phenyl-1H-pyrazol-3-yl]benzoic acid (15k)

The compound was synthesized from methyl-4-[4-[2-(benzyloxyamino)-2-oxo-ethyl]-5-phenyl-1H-pyrazol-3-yl]benzoate (396 mg, 0.90 mmol) and BBr_3 (1 M in DCM, 9 ml, 8.97 mmol) according to method A as described above. Yield: 16.2 mg (5%); ESI-MS m/z : 338.3 $[\text{M}+\text{H}]^+$; HPLC: rt 9.41 min (95.5%); ^1H NMR (400 MHz, DMSO-d_6): δ 3.67 (br s, 0.2H), 7.41-7.44 (m, 1H), 7.49 (t, 2H, $^3\text{J}=7.5$ Hz), 7.65 (d, 2H, $^3\text{J}=7.6$ Hz), 7.79 (d, 2H, $^3\text{J}=8.1$ Hz), 8.01-8.05 (m, 2H), 8.91 (br s, 0.9H), 9.26 (br s, 0.1H), 10.13 (br s, 0.1H), 10.66 (s, 0.9H), 13.16 (br s, 1H) mixture of *cis-trans* isomers; HRMS m/z : 338.1134 $[\text{M}+\text{H}]^+$; calcd for $\text{C}_{18}\text{H}_{16}\text{N}_3\text{O}_4^+$: 338.1135.

2-[3-(4-Chloro-2-fluoro-3-hydroxyphenyl)-5-phenyl-1H-pyrazol-4-yl]ethanehydroxamic acid (15l)

The compound was synthesized from *N*-benzyloxy-2-[3-(4-chloro-2-fluoro-3-methoxy-phenyl)-5-phenyl-1H-pyrazol-4-yl]acetamide (80 mg, 0.17 mmol) and BBr_3 (1 M in DCM, 1 ml, 1.03 mmol) according to method A as described above. Yield: 28 mg (45%); ESI-MS m/z : 362.2 $[\text{M}+\text{H}]^+$; HPLC (Gradient A): rt 10.32 min (97.0%); ^1H NMR (400 MHz, DMSO-d_6): δ 3.24 (s, 1.8H), 3.55 (br s, 0.2H), 7.00 (t, 1H, $^3\text{J}=7.8$ Hz), 7.26-7.29 (m, 1H), 7.38-7.42 (m, 1H), 7.47 (t, 2H, $^3\text{J}=7.3$ Hz), 7.66 (d, 2H, $^3\text{J}=7.3$ Hz), 9.92 (br s, 0.1H), 10.45 (br s, 1.9H) mixture of *cis-trans* isomers; HRMS m/z : 362.0699 $[\text{M}+\text{H}]^+$; calcd for $\text{C}_{17}\text{H}_{14}\text{ClFN}_3\text{O}_3^+$: 362.0702.

2-[3-(3-Chloro-5-fluoro-4-hydroxyphenyl)-5-phenyl-1H-pyrazol-4-yl]ethanehydroxamic acid (15m)

The compound was synthesized from *N*-benzyloxy-2-[3-(3-chloro-5-fluoro-4-methoxy-phenyl)-5-phenyl-1H-pyrazol-4-yl]acetamide (100 mg, 0.21 mmol) and BBr_3 (1 M in DCM, 1.3 ml, 1.29 mmol) according to method A as described above. Yield: 13 mg (17%); ESI-MS m/z : 362.3 $[\text{M}+\text{H}]^+$; HPLC: rt 10.51 min (95.9%); ^1H NMR (400 MHz, DMSO-d_6): δ 3.30 (s, 1.8H), 3.61 (s, 0.2H), 7.39-7.44 (m, 1H), 7.46-7.52 (m, 4H), 7.60 (d, 2H, $^3\text{J}=7.3$ Hz), 10.57 (br s, 1H), 10.69 (s, 0.9H), 10.92 (s, 0.1H) mixture of *cis-trans* isomers; HRMS m/z : 362.0699 $[\text{M}+\text{H}]^+$; calcd for $\text{C}_{17}\text{H}_{14}\text{ClFN}_3\text{O}_3^+$: 362.0702.

2-[3-(3-Hydroxyisoxazol-5-yl)-5-phenyl-1H-pyrazol-4-yl]ethanehydroxamic acid (15n)

The compound was synthesized from *N*-benzyloxy-2-[3-(3-benzyloxyisoxazol-5-yl)-5-phenyl-1H-pyrazol-4-yl]acetamide (100 mg, 0.21 mmol) and BBr₃ (1 M in DCM, 1.2 ml, 1.25 mmol) according to method A as described above. Yield: 10 mg (16%); ESI-MS *m/z*: 301.3 [M+H]⁺; HPLC: *rt* 8.37 min (>99%); ¹H NMR (400 MHz, DMSO-*d*₆): δ 3.44 (s, 1.8H), 3.76 (s, 0.2H), 6.16-6.25 (m, 1H), 7.43-7.47 (m, 1H), 7.49-7.53 (m, 2H), 7.61-7.63 (m, 2H), 10.08 (br s, 0.1H), 10.63 (s, 0.9H), 11.37 (br s, 1H) mixture of *cis-trans* isomers; HRMS *m/z*: 301.0929 [M+H]⁺; calcd for C₁₄H₁₃N₄O₄⁺: 301.0931.

2-[5-Phenyl-3-[3-(trifluoromethyl)-1H-pyrazol-4-yl]-1H-pyrazol-4-yl]ethanehydroxamic acid (15o)

The compound was synthesized from *N*-benzyloxy-2-[3-[1-*tert*-butyl-3-(trifluoromethyl)pyrazol-4-yl]-5-phenyl-1H-pyrazol-4-yl]acetamide (120 mg, 0.24 mmol) and BBr₃ (1 M in DCM, 965 μl, 0.96 mmol) according to method A as described above. Yield: 26 mg (30%); ESI-MS *m/z*: 352.2 [M+H]⁺; HPLC: *rt* 9.84 min (97.9%); ¹H NMR (400 MHz, DMSO-*d*₆): δ 3.21 (s, 1.8H), 3.52 (br s, 0.2H), 7.39-7.42 (m, 1H), 7.48 (t, 2H, ³J=7.7 Hz), 7.64-7.66 (m, 2H), 8.07 (s, 1H), 10.00 (br s, 0.1H), 10.55 (s, 0.9H), 13.77 (br s, 1H) mixture of *cis-trans* isomers; HRMS *m/z*: 352.1013 [M+H]⁺; calcd for C₁₅H₁₃F₃N₅O₂⁺: 352.1016.

2-[5-Phenyl-3-[3-(1H-tetrazol-5-yl)phenyl]-1H-pyrazol-4-yl]ethanehydroxamic acid (15p)

The compound was synthesized from *N*-benzyloxy-2-[3-[3-[1-[(4-methoxyphenyl)methyl]-tetrazol-5-yl]phenyl]-5-phenyl-1H-pyrazol-4-yl]acetamide (188 mg, 0.33 mmol) and BBr₃ (1 M in DCM, 1.3 ml, 1.32 mmol) according to method A as described above. Yield: 38 mg (32%); ESI-MS *m/z*: 362.1 [M+H]⁺; HPLC: *rt* 9.47 min (>99%); ¹H NMR (400 MHz, DMSO-*d*₆): δ 3.40 (s, 1.7H), 3.66 (br s, 0.3H), 7.41-7.45 (m, 1H), 7.51 (t, 2H, ³J=7.5 Hz), 7.64-7.72 (m, 3H), 7.86-7.88 (m, 1H), 8.04-8.06 (m, 1H), 8.37 (s, 1H), 10.11 (br s, 0.1H), 10.62 (s, 0.9H) mixture of *cis-trans* isomers; HRMS *m/z*: 362.1356 [M+H]⁺; calcd for C₁₈H₁₆N₇O₂⁺: 362.1360.

***cis*-2-[4-[2-(Hydroxyamino)-2-oxo-ethyl]-5-phenyl-1H-pyrazol-3-yl]cyclohexanecarboxylic acid (15q)**

The compound was synthesized from *cis*-2-[4-[2-(benzyloxyamino)-2-oxo-ethyl]-5-phenyl-1H-pyrazol-3-yl]cyclohexanecarboxylic acid (147 mg, 0.34 mmol) and BBr₃ (1 M in DCM, 3.4 ml, 3.39 mmol) according to method A as described above. Yield: 2 mg (2%); ESI-MS m/z: 344.2 [M+H]⁺; HPLC: rt 9.01 min (95.6%); ¹H NMR (400 MHz, DMSO-d₆): δ 1.35-1.40 (m, 3H), 1.60-1.75 (m, 3.5H), 1.78-1.87 (m, 0.5H), 1.99-2.07 (m, 1H), 2.18 (br s, 1H), 2.76-2.74 (m, 1H), 3.17-3.30 (m, 2H), 7.33-7.37 (m, 1H), 7.41-7.45 (m, 2H), 7.48-7.50 (m, 0.2H), 7.61-7.62 (m, 1.8H), 10.52 (br s, 0.2H), 10.50 (s, 0.7H) mixture of *cis-trans* isomers; HRMS m/z: 344.1599 [M+H]⁺; calcd for C₁₈H₂₂N₃O₄⁺: 344.1605.

3-[4-[2-(Hydroxyamino)-2-oxo-ethyl]-5-phenyl-1H-pyrazol-3-yl]cyclohexanecarboxylic acid (15r)

The compound was synthesized from methyl-3-[4-[2-(benzyloxyamino)-2-oxo-ethyl]-5-phenyl-1H-pyrazol-3-yl]cyclohexanecarboxylate (175 mg, 0.39 mmol) and BBr₃ (1 M in DCM, 3.9 ml, 3.91 mmol) according to method A as described above. Yield: 11 mg (8%); ESI-MS m/z: 344.3 [M+H]⁺; HPLC: rt 8.64 min (96.5%); ¹H NMR (400 MHz, DMSO-d₆): 1.26-1.49 (m, 3H), 1.55-1.64 (m, 1H), 1.79-1.85 (m, 2H), 1.92-2.01 (m, 2H), 2.32-2.38 (m, 1H), 2.74-2.78 (m, 1H), 3.22 (s, 2H), 7.33-7.37 (m, 1H), 7.43 (t, 2H, ³J=7.4 Hz), 7.65-7.67 (m, 2H), 9.99 (br s, 0.1H), 10.67 (s, 0.9H) mixture of *cis-trans* isomers; HRMS m/z: 344.1598 [M+H]⁺; calcd for C₁₈H₂₂N₃O₄⁺: 344.1605.

***trans*-4-[4-[2-(Hydroxyamino)-2-oxo-ethyl]-5-phenyl-1H-pyrazol-3-yl]cyclohexanecarboxylic acid (15s)**

The compound was synthesized from *trans*-methyl-4-[4-[2-(benzyloxyamino)-2-oxo-ethyl]-5-phenyl-1H-pyrazol-3-yl]cyclohexanecarboxylate (85 mg, 0.19 mmol) and BBr₃ (1 M in DCM, 1.9 ml, 1.90 mmol) according to method A as described above. Yield: 8 mg (12%); ESI-MS m/z: 344.3 [M+H]⁺; HPLC: rt 8.69 min (>99%); ¹H NMR (400 MHz, CD₃OD): 1.52-1.73 (m, 4H), 2.07-2.17 (m, 4H), 2.39-2.45 (m, 1H), 2.81-2.87 (m, 1H), 3.42 (s, 1.8H), 3.79 (s, 0.2H), 7.45-7.54 (m, 3H), 7.58-7.59 (m, 0.2H), 7.63-7.66 (m, 1.8H) mixture of *cis-trans* isomers; HRMS m/z: 344.1600 [M+H]⁺; calcd for C₁₈H₂₂N₃O₄⁺: 344.1605.

***cis*-4-[4-[2-(Hydroxyamino)-2-oxo-ethyl]-5-phenyl-1H-pyrazol-3-yl]cyclohexanecarboxylic acid (15t)**

The compound was synthesized from *cis*-methyl-4-[4-[2-(benzyloxyamino)-2-oxo-ethyl]-5-phenyl-1H-pyrazol-3-yl]cyclohexanecarboxylate (103 mg, 0.23 mmol) and BBr₃ (1 M in DCM, 2.3 ml, 2.30 mmol) according to method A as described above. Yield: 10 mg (13%); ESI-MS *m/z*: 344.2 [M+H]⁺; HPLC: *rt* 8.67 min (>99%); ¹H NMR (400 MHz, DMSO-*d*₆): 1.40-1.66 (m, 5H), 1.83-1.87 (m, 1H), 1.95-2.01 (m, 1H), 2.10-2.13 (m, 1H), 2.19-2.25 (m, 0.5H), 2.60-2.71 (m, 1.5H), 3.19 (s, 1.8H), 3.53 (br s, 0.2H), 7.33-7.36 (m, 1H), 7.40-7.44 (m, 2H), 7.50-7.53 (m, 0.2H), 7.64-7.68 (m, 1.8H), 9.98 (br s, 0.1H), 10.59-10.62 (0.9H) mixture of *cis-trans* isomers; HRMS *m/z*: 344.1598 [M+H]⁺; calcd for C₁₈H₂₂N₃O₄⁺: 344.1605.

2-[3,5-Bis(1,3-benzodioxol-5-yl)-1H-pyrazol-4-yl]ethanehydroxamic acid (16a)

The compound was synthesized from *N*-benzyloxy-2-[3,5-bis(1,3-benzodioxol-5-yl)-1H-pyrazol-4-yl]acetamide (290 mg, 0.62 mmol) according to method C as described above. Yield: 30 mg (13%); ESI-MS *m/z*: 382.3 [M+H]⁺; HPLC: *rt* 10.72 min (95.4%); ¹H NMR (400 MHz, DMSO-*d*₆): δ 3.26 (s, 1.9H), 3.56 (br s, 0.1H), 6.08 (s, 4H), 6.99-7.01 (m, 2H), 7.08-7.10 (m, 2H), 7.16-7.17 (m, 2H), 10.12 (br s, 0.1H), 10.63 (s, 0.9H) mixture of *cis-trans* isomers; HRMS *m/z*: 382.1028 [M+H]⁺; calcd for C₁₉H₁₆N₃O₆⁺: 382.1034.

3-[3-(3-Carboxyphenyl)-4-[2-(hydroxyamino)-2-oxo-ethyl]-1H-pyrazol-5-yl]benzoic acid (16b)

The compound was synthesized from methyl-3-[4-[2-(benzyloxyamino)-2-oxo-ethyl]-3-(3-methoxycarbonylphenyl)-1H-pyrazol-5-yl]benzoate (150 mg, 0.30 mmol) and BBr₃ (1 M in DCM, 4.5 ml, 4.50 mmol) according to method A as described above. Yield: 3 mg (3%); ESI-MS *m/z*: 382.3 [M+H]⁺; HPLC: *rt* 8.72 min (>99%); ¹H NMR (400 MHz, DMSO-*d*₆): δ 3.37 (s, 1.8H), 3.66 (s, 0.2H), 7.61 (t, 2H, ³J=7.8 Hz), 7.87-7.89 (m, 2H), 7.96-7.98 (m, 2H), 8.20-8.25 (m, 2H), 10.13 (br s, 0.1H), 10.61 (s, 0.9H) mixture of *cis-trans* isomers; HRMS *m/z*: 382.1036 [M+H]⁺; calcd for C₁₉H₁₆N₃O₆⁺: 382.1034.

4-[3-(4-Carboxyphenyl)-4-[2-(hydroxyamino)-2-oxo-ethyl]-1H-pyrazol-5-yl]benzoic acid (16c)

The compound was synthesized from methyl-4-[4-[2-(benzyloxyamino)-2-oxo-ethyl]-3-(4-methoxycarbonylphenyl)-1H-pyrazol-5-yl]benzoate (100 mg, 0.20 mmol) and BBr_3 (1 M in DCM, 2 ml, 2 mmol) according to method A as described above. Yield: 3 mg (3%); ESI-MS m/z : 382.2 $[\text{M}+\text{H}]^+$; HPLC: rt 8.43 min (96.4%); ^1H NMR (400 MHz, CD_3OD): δ 3.49 (s, 2H), 7.74-7.76 (m, 4H), 8.09-8.14 (m, 4H); HRMS m/z : 382.1030 $[\text{M}+\text{H}]^+$; calcd for $\text{C}_{19}\text{H}_{16}\text{N}_3\text{O}_6^+$: 382.1034.

2-[3,5-Bis(4-chloro-2-fluoro-3-hydroxyphenyl)-1H-pyrazol-4-yl]ethanehydroxamic acid (16d)

The compound was synthesized from *N*-benzyloxy-2-[3,5-bis(4-chloro-2-fluoro-3-methoxy-phenyl)-1H-pyrazol-4-yl]acetamide (50 mg, 0.09 mmol) and BBr_3 (1 M in DCM, 912 μl , 0.91 mmol) according to method A as described above. Yield: 4 mg (11%); ESI-MS m/z : 430.3 $[\text{M}+\text{H}]^+$; HPLC: rt 10.40 min (96.8%); ^1H NMR (400 MHz, $\text{DMSO}-d_6$): δ 3.15 (s, 1.8H), 3.47 (br s, 0.2H), 6.99-7.03 (m, 2H), 7.26-7.29 (m, 2H), 9.76 (br s, 0.1H), 10.31 (s, 0.9H), 10.50 (br s, 2H) mixture of *cis-trans* isomers; HRMS m/z : 430.0164 $[\text{M}+\text{H}]^+$; calcd for $\text{C}_{17}\text{H}_{12}\text{Cl}_2\text{F}_2\text{N}_3\text{O}_4^+$: 430.0167.

3-[3-(1,3-Benzodioxol-5-yl)-4-[2-(hydroxyamino)-2-oxo-ethyl]-1H-pyrazol-5-yl]benzoic acid (16e)

The compound was synthesized from methyl-3-[3-(1,3-benzodioxol-5-yl)-4-[2-(benzyloxyamino)-2-oxo-ethyl]-1H-pyrazol-5-yl]benzoate (180 mg, 0.37 mmol) and lithium hydroxide monohydrate (31 mg, 0.74 mmol) according to method B and C as described above. Yield: 90 mg (69%); ESI-MS m/z : 382.3 $[\text{M}+\text{H}]^+$; HPLC: rt 9.63 min (>99%); ^1H NMR (400 MHz, $\text{DMSO}-d_6$): δ 3.32 (s, 1.8H), 3.61 (br s, 0.2H), 6.09 (s, 2H), 7.02-7.04 (m, 1H), 7.10-7.13 (m, 1H), 7.19-7.20 (m, 1H), 7.58 (t, 1H, $^3J=7.7$ Hz), 7.84-7.86 (m, 1H), 7.94-7.96 (m, 1H), 8.18-8.24 (m, 1H), 10.13 (br s, 0.1H), 10.62 (s, 0.9H) mixture of *cis-trans* isomers; HRMS m/z : 382.1029 $[\text{M}+\text{H}]^+$; calcd for $\text{C}_{19}\text{H}_{16}\text{N}_3\text{O}_6^+$: 382.1034.

4-[3-(1,3-Benzodioxol-5-yl)-4-[2-(hydroxyamino)-2-oxo-ethyl]-1H-pyrazol-5-yl]benzoic acid (16f)

The compound was synthesized from methyl-4-[3-(1,3-benzodioxol-5-yl)-4-[2-(benzyloxyamino)-2-oxo-ethyl]-1H-pyrazol-5-yl]benzoate (160 mg, 0.33 mmol) and lithium hydroxide monohydrate (28 mg, 0.66 mmol) according to method B and C as described above. Yield: 8 mg (10%); ESI-MS m/z : 382.2 $[\text{M}+\text{H}]^+$; HPLC: rt 9.68 min (>99%); ^1H NMR (400 MHz, $\text{DMSO}-d_6$): δ 3.33 (s, 1.8H), 3.63 (br s,

0.2H), 6.09 (s, 2H), 7.02-7.04 (m, 1H), 7.12-7.14 (m, 1H), 7.21-7.22 (m, 1H), 7.75-7.77 (m, 2H), 8.00-8.02 (m, 2H), 10.14 (br s, 0.1H), 10.66 (s, 0.9H) mixture of *cis-trans* isomers; HRMS m/z: 382.1030 [M+H]⁺; calcd for C₁₉H₁₆N₃O₆⁺: 382.1034.

3-[3-(4-Carboxyphenyl)-4-[2-(hydroxyamino)-2-oxo-ethyl]-1H-pyrazol-5-yl]benzoic acid (16g)

The compound was synthesized from methyl-3-[4-[2-(benzyloxyamino)-2-oxo-ethyl]-3-(4-methoxycarbonylphenyl)-1H-pyrazol-5-yl]benzoate (50 mg, 0.10 mmol) and BBr₃ (1 M in DCM, 1.5 ml, 1.50 mmol) according to method A described above. Yield: 3 mg (7%); ESI-MS m/z: 382.3 [M+H]⁺; HPLC: rt 8.64 min (>99%); ¹H NMR (400 MHz, CD₃OD): δ 3.49 (s, 1.8H), 3.82 (br s, 0.2H), 7.60 (t, 1H, ³J=7.8 Hz), 7.75-7.77 (m, 2H), 7.87-7.89 (m, 1H), 8.07-8.14 (m, 3H), 8.30 (s, 1H) mixture of *cis-trans* isomers; HRMS m/z: 382.1033 [M+H]⁺; calcd for C₁₉H₁₆N₃O₆⁺: 382.1034.

4-[5-(4-Chloro-2-fluoro-3-hydroxy-phenyl)-4-[2-(hydroxyamino)-2-oxo-ethyl]-1H-pyrazol-3-yl]benzoic acid (16h)

The compound was synthesized from methyl-4-[4-[2-(benzyloxyamino)-2-oxo-ethyl]-5-(4-chloro-2-fluoro-3-methoxy-phenyl)-1H-pyrazol-3-yl]benzoate (90 mg, 0.17 mmol) and BBr₃ (1 M in DCM, 2.1 ml, 2.06 mmol) according to method A described above. Yield: 4 mg (5%); ESI-MS m/z: 406.3 [M+H]⁺; HPLC: rt 9.63 min (>99%); ¹H NMR (400 MHz, MeCN-d₃): δ 3.40 (s, 1.8H), 3.74 (br s, 0.2H), 6.97-7.01 (m, 1H), 7.21-7.24 (m, 1H), 7.76-7.78 (m, 2H), 8.11-8.13 (m, 2H) mixture of *cis-trans* isomers; HRMS m/z: 406.0597 [M+H]⁺; calcd for C₁₈H₁₄ClFN₃O₅⁺: 406.0601.

3-[5-(4-Chloro-2-fluoro-3-hydroxy-phenyl)-4-[2-(hydroxyamino)-2-oxo-ethyl]-1H-pyrazol-3-yl]benzoic acid (16i)

The compound was synthesized from methyl-3-[4-[2-(benzyloxyamino)-2-oxo-ethyl]-5-(4-chloro-2-fluoro-3-methoxy-phenyl)-1H-pyrazol-3-yl]benzoate (30 mg, 0.06 mmol) and BBr₃ (1 M in DCM, 687 μl, 0.69 mmol) according to method A described above. Yield: 4 mg (16%); ESI-MS m/z: 406.3 [M+H]⁺; HPLC: rt 9.55 min (95.3%); ¹H NMR (400 MHz, DMSO-d₆): δ 3.26 (s, 2H), 6.97-7.01 (m, 1H), 7.28-7.30 (m, 1H), 7.57-7.61 (m, 1H), 7.90-7.92 (m, 1H), 7.95-7.97 (m, 1H), 8.21-8.27 (m,

1H), 9.95 (br s, 0.1H), 10.45 (s, 0.7H), 10.53 (br s, 0.5H) mixture of *cis-trans* isomers; HRMS m/z: 406.0597 [M+H]⁺; calcd for C₁₈H₁₄ClFN₃O₅⁺: 406.0601.

3-[5-(3-Chloro-5-fluoro-4-hydroxy-phenyl)-4-[2-(hydroxyamino)-2-oxo-ethyl]-1H-pyrazol-3-yl]benzoic acid (16j)

The compound was synthesized from methyl-3-[4-[2-(benzyloxyamino)-2-oxo-ethyl]-5-(3-chloro-5-fluoro-4-methoxy-phenyl)-1H-pyrazol-3-yl]benzoate (90 mg, 0.17 mmol) and BBr₃ (1 M in DCM, 2.1 ml, 2.06 mmol) according to method A described above. Yield: 18 mg (26%); ESI-MS m/z: 406.3 [M+H]⁺; HPLC: rt 9.55 min (97.6%); ¹H NMR (400 MHz, DMSO-d₆): δ 3.33 (s, 1.8H), 3.63 (br s, 0.2H), 7.47-7.52 (m, 2H), 7.60 (t, 1H, ³J=7.8 Hz), 7.83-7.84 (m, 1H), 7.96-7.98 (m, 1H), 8.16-8.22 (m, 1H), 10.19 (br s, 0.1H), 10.62-10.68 (m, 1.9H) mixture of *cis-trans* isomers; HRMS m/z: 406.0593 [M+H]⁺; calcd for C₁₈H₁₄ClFN₃O₅⁺: 406.0601.

3-[4-[2-(Hydroxyamino)-2-oxo-ethyl]-3-[*cis*-2-carboxycyclohexyl]-1H-pyrazol-5-yl]benzoic acid (16k)

The compound was synthesized from *cis*-2-[4-[2-(benzyloxyamino)-2-oxo-ethyl]-5-(3-methoxycarbonylphenyl)-1H-pyrazol-3-yl]cyclohexanecarboxylic acid (154 mg, 0.31 mmol) and lithium hydroxide monohydrate (26 mg, 0.63 mmol) according to method B and C as described above. Yield: 37 mg (36%); ESI-MS m/z: 388.3 [M+H]⁺; HPLC: rt 8.77 min (96.5%); ¹H NMR (400 MHz, DMSO-d₆): δ 1.37-1.39 (m, 2H), 1.63-1.73 (m, 4H), 2.08-2.18 (m, 2H), 2.68-2.76 (m, 1H), 3.20-3.29 (m, 3H), 7.56 (t, 1H, ³J=7.7 Hz), 7.89-7.93 (m, 2H), 8.23 (s, 1H), 10.03 (br s, 0.2H), 10.62 (s, 0.8H) mixture of *cis-trans* isomers; HRMS m/z: 388.1499 [M+H]⁺; calcd for C₁₉H₂₂N₃O₆⁺: 388.1503.

3-[3-(*trans*-4-Carboxycyclohexyl)-4-[2-(hydroxyamino)-2-oxo-ethyl]-1H-pyrazol-5-yl]benzoic acid (16l)

The compound was synthesized from methyl-3-[4-[2-(benzyloxyamino)-2-oxo-ethyl]-3-(*trans*-4-methoxycarbonylcyclohexyl)-1H-pyrazol-5-yl]benzoate (216 mg, 0.43 mmol) and BBr₃ (1 M in DCM, 8.1 ml, 8.11 mmol) according to method A described above. Yield: 2 mg (1%); ESI-MS m/z: 388.3 [M+H]⁺; HPLC: rt 7.95 min (>99%); ¹H NMR (400 MHz, CD₃OD): 1.43-1.73 (m, 4H), 2.04-2.16 (m,

4H), 2.38-2.44 (m, 1H), 2.78-2.83 (m, 1H), 3.41 (s, 1.4H), 3.67 (s, 0.6H), 7.59 (t, 1H, $^3J=7.6$ Hz), 7.88-7.93 (m, 1H), 8.07-8.09 (m, 1H), 8.29 (s, 1H) mixture of *cis-trans* isomers; HRMS m/z : 388.1501 $[M+H]^+$; calcd for $C_{19}H_{22}N_3O_6^+$: 388.1503.

3-[3-(*cis*-4-Carboxycyclohexyl)-4-[2-(hydroxyamino)-2-oxo-ethyl]-1H-pyrazol-5-yl]benzoic acid (16m)

The compound was synthesized from methyl-3-[4-[2-(benzyloxyamino)-2-oxo-ethyl]-3-(*cis*-4-methoxycarbonylcyclohexyl)-1H-pyrazol-5-yl]benzoate (185 mg, 0.37 mmol) and BBR_3 (1 M in DCM, 7.0 ml, 6.95 mmol) according to method A described above. Yield: 2 mg (2%); ESI-MS m/z : 388.3 $[M+H]^+$; HPLC: rt 8.00 min (95.2%); 1H -NMR (400 MHz, CD_3OD): δ 1.57-1.73 (m, 4H), 2.04-2.15 (m, 4H), 2.38-2.48 (m, 1H), 2.77-2.83 (m, 1H), 3.41 (s, 1.7H), 3.66 (s, 0.3H), 7.58 (t, 1H, $^3J=7.6$ Hz), 7.88-7.90 (m, 1H), 8.06-8.08 (m, 1H), 8.29 (s, 1H) mixture of *cis-trans* isomers; HRMS m/z : 388.1502 $[M+H]^+$; calcd for $C_{19}H_{22}N_3O_6^+$: 388.1503.

General methods for the synthesis of *N*-substituted 3,5-diphenylpyrazole derivatives 19a-f, 20, 24a-c

Method A: The respective diphenylpyrazole (1 equiv) was dissolved in DMF (5 ml), cooled down to 0 °C and treated with NaH (60% dispersion in mineral oil, 1.2-1.5 equiv). After 30 minutes the mixture was allowed to warm up to room temperature and stirred overnight. The reaction mixture was quenched with water and extracted with EtOAc (3x25 ml). The combined organic layers were dried over Na_2SO_4 and evaporated. The residue was purified by flash chromatography (silica, heptane/EtOAc).

Method B: The respective diphenylpyrazole (1 equiv) was dissolved in DCM ($c=0.1$ M) and the respective boronic acid (2 equiv), triethylamine (2 equiv), $Cu(OAc)_2$ (1.5 equiv) and molecular sieve (3Å) were added. The mixture was stirred at room temperature and under atmospheric oxygen. After 72 hours the mixture was filtered through celite and evaporated. The residue was purified by flash chromatography (silica, heptane/EtOAc).

General method for the synthesis of hydroxamic acids from carboxylic acid esters 21a, 21e-i, 22

The respective ester derivative (1 equiv) was dissolved in dry MeOH (5 ml) and treated with NaOCH₃ (5 N, 6 equiv) and hydroxylamine hydrochloride (3 equiv). The mixture was heated at 80 °C for 10 minutes in a microwave. After cooling, the volatiles were evaporated. The remains were taken up in a small amount of water and the pH was adjusted to ~8 by means of diluted HCl. The aqueous layer was extracted with EtOAc (3x25 ml), the combined organic layers were dried over Na₂SO₄, filtered and evaporated to dryness. The residue was purified by semi-preparative HPLC.

2-(1-Methyl-3,5-diphenyl-pyrazol-4-yl)ethanehydroxamic acid (21a)

The compound was synthesized from methyl-2-(1-methyl-3,5-diphenyl-pyrazol-4-yl)acetate (210 mg, 0.69 mmol), NaOCH₃ (5 N, 823 μl, 4.11 mmol) and hydroxylamine hydrochloride (143 mg, 2.06 mmol). Yield: 96 mg (45%); ESI-MS m/z: 308.2 [M+H]⁺; HPLC: rt 11.55 min (>99%); ¹H NMR (400 MHz, DMSO-d₆): δ 3.14 (s, 1.8H), 3.45 (s, 0.2H), 3.77 (s, 3H), 7.33-7.37 (m, 1H), 7.42 (t, 2H, ³J=7.5 Hz), 7.47-7.57 (m, 5H), 7.64-7.67 (m, 2H), 10.00 (s, 0.1H), 10.45 (s, 0.9H) mixture of *cis-trans* isomers; HRMS m/z: 308.1407 [M+H]⁺; calcd for C₁₈H₁₈N₃O₂⁺: 308.1394.

2-(1-Benzyl-3,5-diphenyl-pyrazol-4-yl)ethanehydroxamic acid (21e)

The compound was synthesized from methyl-2-(1-benzyl-3,5-diphenyl-pyrazol-4-yl)acetate (230 mg, 0.60 mmol), NaOCH₃ (5 N, 722 μl, 3.61 mmol) and hydroxylamine hydrochloride (125 mg, 1.80 mmol). Yield: 81 mg (35%); ESI-MS m/z: 384.3 [M+H]⁺, 406.2 [M+Na]⁺; HPLC: rt 15.63 min (>99%); ¹H NMR (400 MHz, DMSO-d₆): 3.18 (s, 1.8H), 3.47 (s, 0.2H), 5.28 (s, 2H), 7.01-7.04 (m, 2H), 7.22-7.31 (m, 3H), 7.22-7.31 (m, 3H); 7.34-7.44 (m, 5H), 7.47-7.51 (m, 3H), 7.8-7.70 (m, 2H), 9.97 (s, 0.1H), 10.45 (s, 0.9H) mixtures of *cis-trans* isomers; HRMS m/z: 384.1726 [M+H]⁺; calcd for C₂₄H₂₂N₃O₂⁺: 384.1707.

2-[1-(1,3-Benzodioxol-5-ylmethyl)-3,5-diphenyl-pyrazol-4-yl]ethanehydroxamic acid (21f)

The compound was synthesized from methyl-2-[1-(1,3-benzodioxol-5-yl-methyl)-3,5-diphenyl-pyrazol-4-yl]acetate (305 mg, 0.72 mmol), NaOCH₃ (858 μl, 4.29 mmol) and hydroxylamine hydrochloride (149 mg, 2.15 mmol). Yield: 161 mg (53%); ESI-MS m/z: 428.4 [M+H]⁺; HPLC: rt

15.33 min (>99%); ¹H NMR (400 MHz, DMSO-d₆): 3.15 (s, 1.8H), 3.46 (s, 0.2H), 5.17 (s, 2H), 5.97 (s, 2H), 6.47-6.49 (m, 1H), 6.56-6.57 (M, 1H), 6.79-6.81 (m, 1H), 7.34-7.44 (m, 5H), 7.48-7.53 (m, 3H), 7.58-7.59 (m, 0.2H), 7.66-7.69 (m, 1.8H), 9.96 (s, 0.1H), 10.44 (s, 0.9H) mixture of *cis-trans* isomers; HRMS m/z: 428.1601 [M+H]⁺; calcd for C₂₅H₂₂N₃O₄⁺: 428.1605.

3-[[4-[2-(Hydroxyamino)-2-oxo-ethyl]-3,5-diphenyl-pyrazol-1-yl]methyl]benzoic acid (21g)

The compound was synthesized from 3-[[4-(2-methoxy-2-oxo-ethyl)-3,5-diphenyl-pyrazol-1-yl]methyl]benzoic acid (311 mg, 0.73 mmol), NaOCH₃ (876 μl, 4.38 mmol) and hydroxylamine hydrochloride (152 mg, 2.19 mmol). Yield: 16 mg (5%); ESI-MS m/z: 428.2 [M+H]⁺, 450.2 [M+Na]⁺; HPLC: rt 12.88 min (>99%); ¹H NMR (400 MHz, DMSO-d₆): 3.17 (s, 1.8H), 3.47 (s, 0.2H), 5.34 (s, 2H), 7.23-7.25 (m, 1H), 7.35-7.50 (m, 9H), 7.58-7.60 (m, 0.3H), 7.67-7.69 (m, 2.7H), 7.81-7.83 (m, 1H), 9.96 (s, 0.1H), 10.45 (s, 0.9H) mixture of *cis-trans* isomers; HRMS m/z: 428.1599 [M+H]⁺; calcd for C₂₅H₂₂N₃O₄⁺: 428.1605.

4-[[4-[2-(Hydroxyamino)-2-oxo-ethyl]-3,5-diphenyl-pyrazol-1-yl]methyl]benzoic acid (21h)

The compound was synthesized from 4-[[4-(2-methoxy-2-oxo-ethyl)-3,5-diphenyl-pyrazol-1-yl]methyl]benzoic acid (400 mg, 0.94 mmol), NaOCH₃ (1.1 ml, 5.63 mmol) and hydroxylamine hydrochloride (196 mg, 2.81 mmol). Yield: 130 mg (32%); ESI-MS m/z: 428.2 [M+H]⁺; HPLC: rt 12.69 min (>99%); ¹H NMR (400 MHz, DMSO-d₆): δ 3.18 (s, 1.8H), 3.48 (s, 0.2H), 5.35 (s, 2H), 7.13-7.15 (m, 2H), 7.35-7.49 (m, 8H), 7.59-7.61 (m, 0.2H), 7.68-7.69 (m, 1.8H), 7.85 (t, 2H, ³J=8.2 Hz), 9.98 (s, 0.1H), 10.45 (s, 0.9H), 12.90 (br s, 1H) mixture of *cis-trans* isomers; HRMS m/z: 428.1600 [M+H]⁺; calcd for C₂₅H₂₂N₃O₄⁺: 428.1605.

2-[1-[(4-Chloro-2-fluoro-3-hydroxy-phenyl)methyl]-3,5-diphenyl-pyrazol-4-yl]ethanehydroxamic acid (21i)

The compound was synthesized from methyl-2-[1-[(4-chloro-2-fluoro-3-methoxy-phenyl)methyl]-3,5-diphenyl-pyrazol-4-yl]acetate (300 mg, 0.65 mmol), NaOCH₃ (774 μl, 3.87 mmol) and hydroxylamine hydrochloride (135 mg, 1.94 mmol). The final deprotection of the phenol was accomplished by treatment with BBr₃ (1 M in DCM, 3 equiv). Yield: 142 mg (54%); ESI-MS m/z: 452.2 [M+H]⁺; HPLC:

rt 14.75 min (98.4%); ¹H NMR (400 MHz, DMSO-d₆): δ 3.15 (s, 1.8H), 3.46 (s, 0.2H), 5.27 (s, 2H), 6.42-6.46 (m, 1H), 7.11-7.13 (m, 1H), 7.34-7.44 (m, 5H), 7.49-7.53 (m, 3H), 7.57-7.58 (m, 0.2H), 7.65-7.67 (m, 1.8H), 9.97 (s, 0.1H), 10.36 (br s, 1H), 10.44 (s, 0.9H) mixture of *cis-trans* isomers; HRMS m/z: 452.1165 [M+H]⁺; calcd for C₂₄H₂₀ClFN₃O₃⁺: 452.1172.

3-[1-[(4-Chloro-2-fluoro-3-hydroxy-phenyl)methyl]-3,5-diphenyl-pyrazol-4-yl]propanehydroxamic acid (22)

The compound was synthesized from methyl-3-[1-[(4-chloro-2-fluoro-3-methoxy-phenyl)methyl]-3,5-diphenyl-pyrazol-4-yl]propanoate (250 mg, 0.52 mmol), NaOCH₃ (626 μl, 3.13 mmol) and hydroxylamine hydrochloride (109 mg, 1.57 mmol). The final deprotection of the phenol was accomplished by treatment with BBr₃ (1 M in DCM, 3 equiv). Yield: 56 mg (23%); ESI-MS m/z: 466.2 [M+H]⁺; HPLC: rt 15.28 min (>99%); ¹H NMR (400 MHz, DMSO-d₆): δ 1.95-1.97 (m, 1.8H), 2.23-2.27 (m, 0.2H), 2.72-2.75 (m, 2H), 5.21 (s, 2H), 6.36 (t, 1H, ³J=7.9 Hz), 7.10 (d, 1H, ³J=8.6 Hz), 7.36-7.38 (m, 3H), 7.45 (t, 2H, ³J=7.5 Hz), 7.49-7.53 (m, 3H), 7.68 (d, 2H, ³J=7.5 Hz), 9.75 (s, 0.1H), 10.26 (s, 0.9H), 10.36 (s, 1H) mixture of *cis-trans* isomers; HRMS m/z: 466.1325 [M+H]⁺; calcd for C₂₅H₂₂ClFN₃O₃⁺: 466.1328.

General method for deprotection of trityl-protected hydroxamic acid derivatives 21b-d

The respective trityl-protected hydroxamic acid derivative (1 equiv) was treated with TFA/DCM (1:1 v/v, 5 ml) and triisopropylsilane (1.5 equiv). The mixture was stirred for 3 hours at room temperature. The volatiles were evaporated and the residue was purified by semi-preparative HPLC.

2-(1,3,5-Triphenylpyrazol-4-yl)ethanehydroxamic acid (21b)

The compound was synthesized from 2-(1,3,5-triphenylpyrazol-4-yl)-*N*-trityloxy-acetamide (150 mg, 0.25 mmol). Yield: 50 mg (55%); ESI-MS: m/z 370.3 [M+H]⁺, 392.2 [M+Na]⁺; HPLC: rt 15.49 min (>99%); ¹H NMR (400 MHz, DMSO-d₆): δ 3.24 (s, 1.8H), 3.54 (s, 0.2H), 7.28-7.42 (m, 11H), 7.45-7.49 (m, 2H), 7.66-7.68 (m, 0.2H), 7.74-7.76 (m, 1.8H), 10.06 (s, 0.1H), 10.53 (s, 0.9H) mixture of *cis-trans* isomers; HRMS m/z: 370.1569 [M+H]⁺; calcd for C₂₃H₂₀N₃O₂⁺: 370.1550.

4-[4-[2-(Hydroxyamino)-2-oxo-ethyl]-3,5-diphenyl-pyrazol-1-yl]benzoic acid (21c)

The compound was synthesized from *tert*-butyl-4-(4-(2-oxo-2-((trityloxy)amino)ethyl)-3,5-diphenyl-1H-pyrazol-1-yl)benzoate (200 mg, 0.28 mmol). Yield: 55 mg (48%); ESI-MS *m/z*: 414.2 [M+H]⁺; HPLC: *rt* 13.08 min (>99%); ¹H NMR (400 MHz, DMSO-*d*₆): δ 3.24 (s, 1.8H), 3.55 (s, 0.2H), 7.28-7.52 (m, 10H), 7.68-7.79 (m, 2H), 7.90-7.92 (m, 2H), 10.09 (s, 0.1H), 10.55 (s, 0.9H) mixture of *cis-trans* isomers; HRMS *m/z*: 414.1466 [M+H]⁺; calcd for C₂₄H₂₀N₃O₄⁺: 414.1448.

3-[4-[2-(Hydroxyamino)-2-oxo-ethyl]-3,5-diphenyl-pyrazol-1-yl]benzoic acid (21d)

The compound was synthesized from *tert*-butyl-3-(4-(2-oxo-2-((trityloxy)amino)ethyl)-3,5-diphenyl-1H-pyrazol-1-yl)benzoate (210 mg, 0.30 mmol). Yield: 45 mg (39%); ESI-MS *m/z*: 414.3 [M+H]⁺; HPLC: *rt* 13.09 min (>99%); ¹H NMR (400 MHz, DMSO-*d*₆): δ 3.25 (s, 1.8H), 3.55 (s, 0.2H), 7.28-7.35 (m, 2H), 7.40-7.50 (m, 8H), 7.67-7.69 (m, 0.2H), 7.75-7.76 (m, 1.8H), 7.83-7.86 (m, 1H), 7.89 (s, 1H), 10.08 (s, 0.1H), 10.53 (s, 0.9H) mixture of *cis-trans* isomers; HRMS *m/z*: 414.1468 [M+H]⁺; calcd for C₂₄H₂₀N₃O₄⁺: 414.1448.

Docking

The docking experiments were performed with GOLD (version 2020.1) in combination with the HERMES visualizer. For the target meprin β the pdb structure PDB ID: 7AQ1 was employed.³³ Only chain A and the corresponding zinc ion were used (monomer). For meprin α the recently reported homology model was utilized.³¹ The active site was defined by the zinc ion and a radius of 15 Å. The ligands were used in their deprotonated forms. For each compound 20 docking runs were performed and scored with ChemScore. The search efficacy was set to 100%. The docking was carried out with a scaffold match constraint to place the ligand onto a given scaffold location within the binding site. The hydroxamic acid substructure of the co-crystallized ligand (PDB ID: 7AQ1) was used as a template for this purpose. Compound 15m was docked in the rigid conformation of meprin α and β. For compound 21i and 22 the side chains of the respective amino acids Y¹⁸⁷ and R²⁴² in S₁- and S₁'-binding site of meprin α were specified as flexible upon docking. The allowed rotamers are defined from a rotamer library.⁴²

Enzymatic Assays

Recombinant human meprin β was expressed in yeast and characterized as previously described.⁴³ Recombinant human meprin α was expressed and purified from insect cells (S2) and characterized analogously. MMP2, 9, 13, ADAM10 and 17 were purchased from a commercial vendor (R&D systems). MMPs were activated prior to measurement by APMA (p-aminophenylmercuric acetate) treatment according to manufacturer's instructions.

The determination of enzymatic activity was based on the cleavage of internally quenched peptide substrates (see supporting information). A typical assay of 100 μ L total volume measured in black 96 half area well plates consisted of 40 μ L buffer, 20 μ L enzyme at a final concentration of 2e-10 M for meprin α and 3e-11 M for meprin β , 20 μ L substrate and 20 μ L inhibitor solution (in buffer, 2% DMSO). Enzymatic activity of ADAMs was measured in 384 well plates with 50 μ L total assay volume consisting of 30 μ L enzyme in buffer, 10 μ L inhibitor and 10 μ L substrate. To ensure reproducibility, the parameters were determined at least in duplicates independently on separate days. For IC₅₀ values the influence of 11 or 14 inhibitor concentrations ranging from 0 to 1e-4 M on the enzymatic activity was investigated in the presence of the respective substrate concentration. Initial velocities were determined and converted into concentration units applying a standard curve obtained after complete conversion of different substrate concentrations under assay conditions. All measurements were performed using a fluorescence plate reader (FLUOstar OPTIMA, BMG Labtech) at 30°C. Depending on the substrates the excitation/emission wavelength was 340/490 nm for enzymatic assays regarding meprin and 340/410 nm for enzymatic assays regarding MMPs and ADAMs. The kinetic data was evaluated using GraphPad Prism (version 5.04, GraphPad Software). Kinetic parameters of inhibition (K_i^{app}) were determined using Morrison's equation.⁴⁴

Cell Viability Assay

Cell viability was assessed in human hepatocellular carcinoma cell line Hep-G2 and in human neuroblastoma cell line SH-SY5Y. Hep-G2 cells were cultivated in RPMI1640 (ThermoFisher) supplemented with 10 % FBS and SH-SY5Y cells were cultivated in DMEM (high-glucose, pyruvate) (ThermoFisher) also supplemented with 10 % FBS in a humidified atmosphere of 37 °C and 5 % CO₂

according to standard cell culture procedures. For the assay, cells were plated in 96-well microtiter plates (Greiner bio-one) at densities of 50.000 cells / well (Hep-G2) and 60.000 cells / well (SH-SY5Y), respectively. After 24 h, compounds dissolved in DMSO are added to fresh medium at concentrations of 30 μ M and 100 μ M (final concentration of DMSO: 1 % (v/v)) and applied to the cells for another 24 h. On the next day, cellular viability is determined using the CytoTox-ONE kit (Promega) based on the viability in control wells incubated with culture medium and 1 % DMSO. In brief, cells were washed two times with PBS. After an incubation with 50 μ l lysis solution (9% w/v of Triton X-100 in water) for 10 min at room temperature following a 10 min incubation with an equal volume of CytoTox-ONE reagent. Stop solution was applied and fluorescence signals were recorded (544 nm / 595 nm) using a CLARIOstar plate reader.

Acknowledgements

We gratefully acknowledge Antje Hamann and Christian Pfennig (IZI-MWT), Dr. Christoph Wiedemann and Dr. Christian Ihling (Martin Luther University, Halle–Wittenberg) for their excellent technical support. Parts of this work were supported by grants from European Regional Development Fund (#ZS/2019/02/97143) and from the German Federal Ministry of Education and Research (#16GW0288K).

Conflict of interest

M. B. is employee of PerioTrap Pharmaceuticals GmbH. C. J. is employee of Vivoryon Therapeutics N.V., Halle (Saale), Germany. The remaining authors declare no competing interests.

References

1. Breig O, Yates M, Neaud V, Couchy G, Grigoletto A, Lucchesi C, Prox J, Zucman-Rossi J, Becker-Pauly C, Rosenbaum J. Metalloproteinase meprin α regulates migration and invasion of human hepatocarcinoma cells and is a mediator of the oncoprotein Reptin. *Oncotarget*. 2017;8(5):7839–51 doi:10.18632/oncotarget.13975.
2. Lottaz D, Maurer CA, Hahn D, Büchler MW, Sterchi EE. Nonpolarized secretion of human meprin alpha in colorectal cancer generates an increased proteolytic potential in the stroma. *Cancer Res*. 1999;59(5):1127–33.
3. Lottaz D, Maurer CA, Noël A, Blacher S, Huguenin M, Nievergelt A, Niggli V, Kern A, Müller S, Seibold F, et al. Enhanced activity of meprin- α , a pro-migratory and pro-angiogenic protease, in colorectal cancer. *PLoS ONE*. 2011;6(11):e26450 doi:10.1371/journal.pone.0026450.
4. Minder P, Bayha E, Becker-Pauly C, Sterchi EE. Meprin α transactivates the epidermal growth factor receptor (EGFR) via ligand shedding, thereby enhancing colorectal cancer cell proliferation and migration. *J Biol Chem*. 2012;287(42):35201–11 doi:10.1074/jbc.M112.368910.
5. OuYang H-Y, Xu J, Luo J, Zou R-H, Chen K, Le Y, Zhang Y-F, Wei W, Guo R-P, Shi M. MEP1A contributes to tumor progression and predicts poor clinical outcome in human hepatocellular carcinoma. *Hepatology*. 2016;63(4):1227–39 doi:10.1002/hep.28397.
6. Wang X, Chen J, Wang J, Yu F, Zhao S, Zhang Y, Tang H, Peng Z. Metalloproteases meprin- α (MEP1A) is a prognostic biomarker and promotes proliferation and invasion of colorectal cancer. *BMC Cancer*. 2016;16:383 doi:10.1186/s12885-016-2460-5.
7. Gao R, Liu D, Guo W, Ge W, Fan T, Li B, Gao P, Liu B, Zheng Y, Wang J. Mep1A enhances TNF-alpha secretion by mast cells and aggravates abdominal aortic aneurysms. *Br. J. Pharmacol*. 2020, 177, 2872-2885. doi:10.1111/bph.15019.
8. Ge W, Hou C, Zhang W, Guo X, Gao P, Song X, Gao R, Liu Y, Guo W, Li B, et al. Mep1a contributes to Ang II-induced cardiac remodeling by promoting cardiac hypertrophy, fibrosis and inflammation. *J Mol Cell Cardiol*. 2020;152:52–68 doi:10.1016/j.yjmcc.2020.11.015.

9. Grainger AT, Pilar N, Li J, Chen M-H, Abramson AM, Becker-Pauly C, Shi W. Identification of Mep1a as a susceptibility gene for atherosclerosis in mice. *Genetics*. 2021;219(4) doi:10.1093/genetics/iyab160.
10. Gellrich A, Scharfenberg F, Peters F, Sammel M, Helm O, Armbrust F, Schmidt F, Lokau J, Garbers C, Sebens S, et al. Characterization of the Cancer-Associated Meprin Beta Variants G45R and G89R. *Front Mol Biosci*. 2021;8:702341 doi:10.3389/fmolb.2021.702341.
11. Schäffler H, Li W, Helm O, Krüger S, Böger C, Peters F, Röcken C, Sebens S, Lucius R, Becker-Pauly C, et al. The cancer-associated meprin β variant G32R provides an additional activation site and promotes cancer cell invasion. *J. Cell Sci*. 2019;132(11):jcs220665 doi:10.1242/jcs.220665.
12. Armbrust F, Colmorgen C, Pietrzik CU, Becker-Pauly C. The Alzheimer's disease associated bacterial protease RgpB from *P. gingivalis* activates the alternative β -secretase meprin β thereby increasing A β generation; bioRxiv 748814; doi: <https://doi.org/10.1101/748814>.
13. Becker-Pauly C, Pietrzik CU. The Metalloprotease Meprin β Is an Alternative β -Secretase of APP. *Front. Mol. Neurosci*. 2017;9:159 doi:10.3389/fnmol.2016.00159.
14. Berner DK, Wessolowski L, Armbrust F, Schneppenheim J, Schlepckow K, Koudelka T, Scharfenberg F, Lucius R, Tholey A, Kleinberger G, et al. Meprin β cleaves TREM2 and controls its phagocytic activity on macrophages. *FASEB J*. 2020 doi:10.1096/fj.201902183R.
15. Bien J, Jefferson T, Causevic M, Jumpertz T, Munter L, Multhaupt G, Weggen S, Becker-Pauly C, Pietrzik CU. The Metalloprotease Meprin Generates Amino Terminal-truncated Amyloid Peptide Species. *J. Biol. Chem*. 2012;287(40):33304–13 doi:10.1074/jbc.M112.395608.
16. Scharfenberg F, Armbrust F, Marengo L, Pietrzik C, Becker-Pauly C. Regulation of the alternative β -secretase meprin β by ADAM-mediated shedding. *Cell. Mol. Life Sci.* 2019;76(16):3193–3206 doi:10.1007/s00018-019-03179-1.
17. Schönherr C, Bien J, Isbert S, Wichert R, Prox J, Altmeppen H, Kumar S, Walter J, Lichtenthaler SF, Weggen S, et al. Generation of aggregation prone N-terminally truncated amyloid β peptides by meprin β depends on the sequence specificity at the cleavage site. *Mol. Neurodegener*. 2016;11(11):19 doi:10.1186/s13024-016-0084-5.

18. Biasin V, Wygrecka M, Marsh LM, Becker-Pauly C, Brcic L, Ghanim B, Klepetko W, Olschewski A, Kwapiszewska G. Meprin β contributes to collagen deposition in lung fibrosis. *Sci. Rep.* 2017;7:39969 doi:10.1038/srep39969.
19. Biasin V, Marsh LM, Egemnazarov B, Wilhelm J, Ghanim B, Klepetko W, Wygrecka M, Olschewski H, Eferl R, Olschewski A, et al. Meprin β , a novel mediator of vascular remodelling underlying pulmonary hypertension. *J Pathol.* 2014;233(1):7–17 doi:10.1002/path.4303.
20. Broder C, Arnold P, Vadon-Le Goff S, Konerding MA, Bahr K, Muller S, Overall CM, Bond JS, Koudelka T, Tholey A, et al. Metalloproteases meprin and meprin are C- and N-procollagen proteinases important for collagen assembly and tensile strength. *Proc Natl Acad Sci U S A.* 2013;110(35):14219–24 doi:10.1073/pnas.1305464110.
21. Banerjee S, Bond JS. Prointerleukin-18 is activated by meprin beta in vitro and in vivo in intestinal inflammation. *J Biol Chem.* 2008;283(46):31371–77 doi:10.1074/jbc.M802814200.
22. Banerjee S, Jin G, Bradley SG, Matters GL, Gailey RD, Crisman JM, Bond JS. Balance of meprin A and B in mice affects the progression of experimental inflammatory bowel disease. *Am J Physiol Gastrointest Liver Physiol.* 2011;300(2):G273-82 doi:10.1152/ajpgi.00504.2009.
23. Herzog C, Seth R, Shah SV, Kaushal GP. Role of meprin A in renal tubular epithelial cell injury. *Kidney Int.* 2007;71(10):1009–18 doi:10.1038/sj.ki.5002189.
24. Herzog C, Haun RS, Kaushal GP. Role of meprin metalloproteinases in cytokine processing and inflammation. *Cytokine.* 2018;114:18–25 doi:10.1016/j.cyto.2018.11.032.
25. Herzog C, Marisiddaiah R, Haun RS, Kaushal GP. Basement membrane protein nidogen-1 is a target of meprin β in cisplatin nephrotoxicity. *Toxicol Lett.* 2015;236(2):110–16 doi:10.1016/j.toxlet.2015.05.005.
26. Kaushal GP, Haun RS, Herzog C, Shah SV. Meprin A metalloproteinase and its role in acute kidney injury. *Am J Physiol Renal Physiol.* 2013;304(9):F1150-8 doi:10.1152/ajprenal.00014.2013.
27. Kruse M-N, Becker C, Lottaz D, Köhler D, Yiallouros I, Krell H-W, Sterchi EE, Stöcker W. Human meprin alpha and beta homo-oligomers: cleavage of basement membrane proteins and

- sensitivity to metalloprotease inhibitors. *Biochem J.* 2004;378(Pt 2):383–89 doi:10.1042/BJ20031163.
28. Madoux F, Tredup C, Spicer TP, Scampavia L, Chase PS, Hodder PS, Fields GB, Becker-Pauly C, Minond D. Development of high throughput screening assays and pilot screen for inhibitors of metalloproteases meprin α and β . *Biopolymers.* 2014;102(5):396–406 doi:10.1002/bip.22527.
 29. Ramsbeck D, Hamann A, Schlenzig D, Schilling S, Buchholz M. First insight into structure-activity relationships of selective meprin β inhibitors. *Bioorg. Med. Chem. Lett.* 2017;27(11):2428–31 doi:10.1016/j.bmcl.2017.04.012.
 30. Ramsbeck D, Hamann A, Richter G, Schlenzig D, Geissler S, Nykiel V, Cynis H, Schilling S, Buchholz M. Structure-Guided Design, Synthesis, and Characterization of Next-Generation Meprin β Inhibitors. *J Med Chem.* 2018;61(10):4578–92 doi:10.1021/acs.jmedchem.8b00330.
 31. Tan K, Jäger C, Schlenzig D, Schilling S, Buchholz M, Ramsbeck D. Tertiary-Amine-Based Inhibitors of the Astacin Protease Meprin α . *ChemMedChem.* 2018;13(16):1619–24 doi:10.1002/cmdc.201800300.
 32. Dufour A, Overall CM. Missing the target: Matrix metalloproteinase antitargets in inflammation and cancer. *Trends Pharmacol. Sci.* 2013;34(4):233–42 doi:10.1016/j.tips.2013.02.004.
 33. Linnert M, Fritz C, Jäger C, Schlenzig D, Ramsbeck D, Kleinschmidt M, Wermann M, Demuth H-U, Parthier C, Schilling S. Structure and Dynamics of Meprin β in Complex with a Hydroxamate-Based Inhibitor. *Int J Mol Sci.* 2021;22(11) doi:10.3390/ijms22115651.
 34. Becker-Pauly C, Barre O, Schilling O, (auf dem Keller, U.), Ohler A, Broder C, Schutte A, Kappelhoff R, Stöcker W, Overall CM. Proteomic Analyses Reveal an Acidic Prime Side Specificity for the Astacin Metalloprotease Family Reflected by Physiological Substrates. *Mol. Cell. Proteom.* 2011;10(9):M111.009233 doi:10.1074/mcp.M111.009233.
 35. Villa JP, Bertenshaw GP, Bond JS. Critical Amino Acids in the Active Site of Meprin Metalloproteinases for Substrate and Peptide Bond Specificity. *J. Biol. Chem.* 2003;278(43):42545–50 doi:10.1074/jbc.M303718200.

36. Hou S, Diez J, Wang C, Becker-Pauly C, Fields GB, Bannister T, Spicer TP, Scampavia LD, Minond D. Discovery and Optimization of Selective Inhibitors of Meprin α (Part I). *Pharmaceuticals*. 2021;14(3) doi:10.3390/ph14030203.
37. Wang C, Diez J, Park H, Spicer TP, Scampavia LD, Becker-Pauly C, Fields GB, Minond D, Bannister TD. Discovery and Optimization of Selective Inhibitors of Meprin α (Part II). *Pharmaceuticals*. 2021;14(3) doi:10.3390/ph14030197.
38. Tan K, Jäger C, Körschgen H, Geissler S, Schlenzig D, Buchholz M, Stöcker W, Ramsbeck D. Heteroaromatic Inhibitors of the Astacin Proteinases Meprin α , Meprin β and Ovastacin Discovered by a Scaffold-Hopping Approach. *ChemMedChem*. 2021;16(6):976–88 doi:10.1002/cmdc.202000822.
39. Heller ST, Natarajan SR. 1,3-diketones from acid chlorides and ketones: a rapid and general one-pot synthesis of pyrazoles. *Org Lett*. 2006;8(13):2675–78 doi:10.1021/ol060570p.
40. Gomis-Rüth FX, Trillo-Muyo S, Stöcker W. Functional and structural insights into astacin metalloproteinases. *Biol. Chem*. 2012;393(10):1027–1041 doi:10.1515/hsz-2012-0149.
41. Riley K, Tran K-A. Strength and Character of R–X $\cdots\pi$ Interactions Involving Aromatic Amino Acid Sidechains in Protein-Ligand Complexes Derived from Crystal Structures in the Protein Data Bank. *Crystals*. 2017;7(9):273. Available from: <https://www.mdpi.com/2073-4352/7/9/273/htm> doi:10.3390/cryst7090273.
42. Lovell SC, Word JM, Richardson JS, Richardson DC. The penultimate rotamer library. *Proteins*. 2000;40(3):389–408 doi:10.1002/1097-0134(20000815)40:3<389:AID-PROT50>3.0.CO;2-2.
43. Schlenzig D, Wermann M, Ramsbeck D, Moenke-Wedler T, Schilling S. Expression, purification and initial characterization of human meprin β from *Pichia pastoris*. *Protein Expr. Purif*. 2015;116:75–81 doi:10.1016/j.pep.2015.08.001.
44. Morrison JF. Kinetics of the reversible inhibition of enzyme-catalysed reactions by tight-binding inhibitors. *Biochim Biophys Acta*. 1969;185(2):269–86 doi:10.1016/0005-2744(69)90420-3.